Kinetic Mechanism of Adenine Nucleotide Binding to and Hydrolysis by the *Escherichia coli* Rep Monomer. 1. Use of Fluorescent Nucleotide Analogues[†]

Keith J. M. Moore and Timothy M. Lohman*

Department of Biochemistry and Molecular Biophysics, Washington University School of Medicine, Box 8231, 660 South Euclid Avenue, St. Louis, Missouri 63110

Received July 15, 1994[⊗]

ABSTRACT: The *Escherichia coli* Rep helicase catalyzes the unwinding of duplex DNA in a reaction that is coupled to ATP binding and hydrolysis. The Rep protein is a stable monomer in the absence of DNA but dimerizes upon binding either single-stranded or duplex DNA, and the dimer appears to be the functionally active form of the Rep helicase. As a first step toward understanding how ATP binding and hydrolysis are coupled energetically to DNA unwinding, we have investigated the kinetic mechanism of nucleotide binding to the Rep monomer (P) using stopped-flow techniques and the fluorescent ATP analogue, 2′(3′)-*O*-(*N*-methylanthraniloyl-ATP (mantATP). The fluorescence of mantATP is enhanced upon Rep binding due to energy transfer from tryptophan. The results are consistent with the following two-step mechanism, in which the bimolecular association step is followed by a conformational change in the P−mantATP complex: $P + mantATP \underset{k_{-1}}{\overset{k_{+1}}{\leftrightarrow}} P\text{−}mantATP \underset{k_{-2}}{\overset{k_{+2}}{\leftrightarrow}} (P\text{−}mantATP)^*$. The following rate and equilibrium constants were determined at 4 °C in 20 mM Tris·HCl (pH 7.5), 6 mM NaCl, 5 mM $MgCl_2$, and 10% (v/v) glycerol: $k_{+1} = (1.1 \pm 0.2) \times 10^7\ M^{-1}\ s^{-1}$; $k_{-1} = 3.2\ (\pm 0.5)\ s^{-1}$; $k_{+2} = 2.9\ (\pm 0.5)\ s^{-1}$; $k_{-2} = 0.04\ (\pm 0.005)\ s^{-1}$; $K_1 = k_{+1}/k_{-1} = (3.4 \pm 0.8) \times 10^6\ M^{-1}$; $K_2 = k_{+2}/k_{-2} = 73\ (\pm 10)$; $K_{overall} = K_1K_2 = (2.30 \pm 0.6) \times 10^8\ M^{-1}$. Similar rate and equilibrium constants are obtained with mantATPγS, whereas the apparent rate constant for mantAMPPNP binding is 15-fold lower than for mantATP and equilibrium binding is weaker ($K_{overall} \sim 10^6\ M^{-1}$). Rep monomer does bind mantATP in the absence of Mg^{2+} ($K_{overall} \sim 5 \times 10^5\ M^{-1}$), although the four rate constants in the above reaction increase by at least 8-fold (k_{-1} and k_{-2} increase by ~100- and ~1000-fold, respectively). The affinities of Mg^{2+} for P−mantATP and (P−mantATP)* are 10- and 1000-fold higher than those for nucleotide-free Rep monomer, indicating that the second step in the reaction is associated with a marked increase in Mg^{2+} affinity. The bound Mg^{2+} in a (P−mantATP)*−Mg^{2+} complex dissociates at a rate that is comparable to the rate of mantATP release. Single-turnover kinetic studies with the Rep monomer indicate a low, but significant, DNA-independent ATPase activity, with a first-order cleavage rate constant of $\sim 10^{-3}\ s^{-1}$ at 4 °C, which increases with temperature ($E_{act} = 18 \pm 2$ kcal mol^{-1}). These results indicate that Rep is a DNA-*stimulated* ATPase rather than a DNA-*dependent* ATPase. The absence of a burst of ADP formation in a multiple ATP turnover experiment suggests that product release is not rate-limiting under these conditions. The approaches described here and in the accompanying paper (Moore & Lohman, 1994) will be useful for subsequent studies of the more complex Rep dimeric species and of other helicases.

DNA helicases are essential enzymes that function in DNA replication, recombination, and repair to catalyze the unwinding of double-stranded DNA (ds-DNA[1]) to yield the single-stranded DNA (ss-DNA) intermediates that are required during these processes [for reviews, see Matson and Kaiser-Rogers (1990), Matson (1991), Lohman (1992, 1993), and Thommes and Hubscher (1992)]. These enzymes function at the junction between ss-DNA and ds-DNA (e.g., at a replication fork) in reactions that require the binding and subsequent hydrolysis of nucleoside 5′-triphosphates (e.g., ATP). Although a large number of these important enzymes have been and continue to be identified, much remains to be uncovered about their mechanisms of action (Lohman, 1992, 1993). In general, helicases that unwind DNA processively must disrupt one or more base pairs within the duplex and then translocate to the next duplex region to repeat the process. This requires that the helicase cycle, vectorially, through a number of energetic (conformational) states in which the affinity for ss-DNA *vs* ds-DNA is altered (Wong & Lohman, 1992). Although it is clear that the coupling of ATP binding and hydrolysis drives the protein through these states in a concerted manner (Hill & Tsuchiya, 1981; Yarranton & Gefter, 1979; Arai et al., 1981a; Wong & Lohman, 1992; Lohman, 1992, 1993), the details of these reactions have yet to be understood.

[†] This work was supported in part by grants to T.M.L. from the American Cancer Society (NP-756B) and the NIH (GM 45948) and by a William M. Keck Foundation Fellowship to K.J.M.M.

* Address correspondence to this author at the Department of Biochemistry and Molecular Biophysics, Washington University School of Medicine, Box 8231, 660 S. Euclid Ave., St. Louis, MO 63110. Telephone: (314)-362-4393. FAX: (314)-362-7183.

[⊗] Abstract published in *Advance ACS Abstracts,* November 1, 1994.

[1] Abbreviations: mantATP, 2′(3′)-*O*-(*N*-methylanthraniloyl)-adenosine 5′-triphosphate; 3′-mant-dATP, 3′-*O*-(*N*-methylanthraniloyl)-2′-deoxyadenosine 5′-triphosphate; other mant-substituted nucleotides and deoxyribonucleotides are abbreviated similarly; AMPPNP, imidoadenosine 5′-triphosphate; ATPγS, adenosine 5′-thiotriphosphate; HPLC, high-performance liquid chromatography; EDTA, ethylenediamine-*N*,*N*,*N*′,*N*′-tetraacetic acid; TEAB, triethylammonium bicarbonate; TLC, thin-layer chromatography; ds-DNA, double-stranded DNA; ss-DNA, single-stranded DNA.

0006-2960/94/0433-14550$04.50/0

An understanding of the mechanism by which a helicase unwinds duplex DNA requires information on the active form (oligomeric state) of the helicase, as well as a quantitative understanding of the energetics and kinetics of its binding to DNA and its interaction with nucleotide cofactors. In this regard, we note that all helicases that have been characterized in any detail appear to function as oligomeric assemblies, some as hexamers and others as dimers. These oligomeric assembly states likely reflect a requirement that the functionally active helicase possesses multiple DNA binding sites (Lohman, 1992, 1993).

We have been studying the *Escherichia coli* Rep helicase in order to understand its mechanism of DNA unwinding. Rep was one of the first enzymes to be identified as a helicase (Scott et al., 1997; Yarranton & Gefter, 1979; Arai & Kornberg, 1981) and has been characterized extensively. Rep is required for DNA unwinding during the replication of several bacteriophages, including ϕX174 (Denhardt et al., 1967; Lane & Denhardt, 1975). Rep appears to function in DNA replication since *rep* mutants show a 50% reduction in the rate of replication fork movement (Lane & Denhardt, 1974, 1975). Although neither Rep nor helicase II (*uvrD* gene product) is an essential *E. coli* gene, *rep/uvrD* double mutants are lethal, indicating that either Rep or helicase II is required for some essential function (Washburn & Kushner, 1991). In this regard, it is interesting that Rep and UvrD can form heterodimers *in vitro* (Wong et al., 1993).

Although Rep remains monomeric (M_r = 76 740)[2] up to at least 12 μM in the absence of DNA (Arai et al., 1981a; Lohman et al., 1989; I. Wong, unpublished data), it forms a homodimer upon binding either ss- or ds-DNA, and the dimer appears to be the active form of the helicase (Chao & Lohman, 1991; Wong et al., 1992; Amaratunga & Lohman, 1993). Determination of the equilibrium constants for DNA binding and Rep dimerization indicates that both subunits of the dimer can bind either ss- or ds-DNA competitively (Wong et al., 1992). ADP and the nonhydrolyzable ATP analogue, imidoadenosine 5′-triphosphate (AMPPNP), affect DNA binding allosterically, such that ADP favors binding of ss-DNA to both subunits, whereas AMPPNP favors simultaneous binding of ss-DNA and ds-DNA to individual subunits of the dimer to form a P_2SD complex (Wong & Lohman, 1992). These experiments and direct unwinding studies (Amaratunga & Lohman, 1993) suggest that the dimeric Rep helicase unwinds DNA by an "active rolling" mechanism in which Rep translocation along DNA is coupled to ATP binding and DNA unwinding is coupled to ATP hydrolysis and that a P_2SD complex is an essential intermediate in the unwinding reaction (Lohman, 1992, 1993; Wong & Lohman, 1992).

Preliminary studies of ATP binding to the Rep monomer, performed by nitrocellulose filter binding in the absence of DNA, indicate that there is one site for ATP per Rep monomer (Arai et al., 1981a), which is consistent with the presence of a putative ATP consensus binding sequence (Walker et al., 1982; Hodgman, 1988). The ATPase activity of Rep protein in the presence of DNA has been examined using steady-state kinetic approaches (Kornberg et al., 1978; Arai et al., 1981a). However, these studies were performed before it was recognized that DNA binding induces Rep dimerization (Chao & Lohman, 1991), and it is clear that dimerization stimulates the steady-state ATPase activity of the Rep protein (Wong et al., 1993).

In order to understand the coupling of ATP binding and hydrolysis to Rep-catalyzed DNA unwinding, we have initiated studies of the kinetics and energetics of nucleotide binding and hydrolysis by the Rep monomer, as well as by the different DNA-ligated Rep dimers. In this report, we have used stopped-flow fluorescence techniques to examine the kinetics and mechanism of nucleotide binding to the Rep monomer, which is present exclusively in the absence of DNA. Since there is no significant change in the intrinsic (tryptophan) fluorescence of Rep monomer upon binding ATP, we have studied the binding of the fluorescent *N*-methylanthraniloyl (mant) derivatives of adenine nucleotides (Hiratsuka, 1983) because there is a substantial increase in mant nucleotide fluorescence upon binding Rep. In the accompanying paper (Moore & Lohman, 1994), we use the fluorescence changes associated with mantATP binding to monitor the kinetics of ATP and ADP binding to Rep by kinetic competition methods. These studies with the Rep monomer provide the basis for future investigations of how the binding of nucleotides (ATP and ADP) is coupled to Rep-catalyzed DNA unwinding.

MATERIALS AND METHODS

Buffers and Rep Protein. Buffers were made with reagent-grade chemicals using distilled H_2O that was deionized using a Milli-Q system (Millipore Corp., Bedford, MA). Unless otherwise stated, all experiments were performed at 4 °C under conditions identical to those used in previous DNA binding studies (Wong et al., 1992; Wong & Lohman, 1992), i.e., 20 mM Tris·HCl (pH 7.5 at 4 °C), 6 mM NaCl, 5 mM $MgCl_2$, and 10% (v/v) glycerol (buffer A). For experiments performed at higher temperatures (e.g., Figure 7), buffer A was titrated to pH 7.5 at each temperature using NaOH. Buffer AE is 20 mM Tris·HCl (pH 7.5 at 4 °C), 6 mM NaCl, 2 mM EDTA, and 10% (v/v) glycerol and was used for experiments conducted in the absence of Mg^{2+}. Rep protein was purified to >99% homogeneity from *E. coli* MZ-1/pRepO (Colasanti & Denhardt, 1987) as described (Lohman et al., 1989; Chao & Lohman, 1991). The Rep concentration was determined spectrophotometrically using $\epsilon_{280} = 7.68 \times 10^4$ M^{-1} cm^{-1} (Amaratunga & Lohman, 1993). Purified Rep protein was stored at −70 °C in 50 mM Tris·HCl (pH 7.5), 0.1 M NaCl, 1 mM EDTA, and 50% (v/v) glycerol, and experiments were initiated within 1 h after removal of the protein from −70 °C. The use of protein that is thawed and stored at −20 °C for reuse, even in 50% glycerol, leads to minor variations in the kinetic rate constants. The results presented here are from experiments performed on three preparations of Rep. Essentially identical rate constants (differing by <15%) were obtained with each preparation.

Nucleotides. The *N*-methylanthraniloyl derivatives of adenine nucleotides (Hiratsuka, 1983) were synthesized and characterized essentially as described (Woodward et al., 1991; Moore et al., 1993). Parent (nonfluorescent) nucleotides were purchased from Sigma (St. Louis, MO). Immediately after synthesis, mant nucleotides were >98% pure, as determined by analytical strong anion exchange (SAX)

[2] The molecular mass of the Rep monomer was calculated from the amino acid sequence of the protein as predicted from the DNA sequence of the *rep* gene (Gilchrist & Denhardt, 1987), as revised by Daniels et al. (1992).

HPLC (Neal et al., 1990; Woodward et al., 1991; Moore et al., 1993). All mant nucleotides were checked for the presence of parent nucleotides by SAX HPLC using a linear gradient system (Moore et al., 1993). Immediately after synthesis, the mant derivatives typically contained <1% parent nucleotide and were repurified when they became <95% pure (typically after ~6 months storage at −70 °C in buffer A). Thio-substituted nucleotides were stored at −70 °C in buffer A containing 50 mM 2-mercaptoethanol. Nucleotide analogues containing a mant fluorophore attached to both the 2′- and 3′-hydroxyl groups (bis-mant derivatives) were obtained as byproducts of the synthesis of the mono-substituted ribonucleotides. They eluted from the preparative DE-52 bicarbonate column (Moore et al., 1993) at ~0.8−0.9 M TEAB, eluted from the isocratic HPLC system at 14 min, and had an A_{256}/A_{356} ratio of 2.7 (ϵ_{356} = 11.6 mM^{-1} cm^{-1}), compared to 4.0 for the singly substituted derivatives. The structure was confirmed by an ion exchange HPLC analysis of samples from a base hydrolysis experiment [analogous to that described by Woodward et al. (1991) with mantATP].

DNA-Independent ATPase Activity of the Rep Monomer. Equal volumes (1 mL) of Rep monomer and [α-^{32}P]ATP in buffer A (final conditions: 0.1−1 μM [α-^{32}P]ATP, 8000 cpm μL^{-1}, 0.2 μM Rep monomer) were mixed manually at 4 °C. After various reaction times, a sample (50 μL) of the reaction mixture was quenched by mixing with 50 μL of 10% (v/v) $HClO_4$ and immediately brought to pH 4 by adding 25 μL of 4 M $NaCH_3CO_2$. Aliquots (1 μL) were subjected to TLC on PEI cellulose and analyzed for ADP as described (Wong et al., 1993). Multiple turnover of mantATP was monitored by HPLC as described (Moore et al., 1993; Woodward et al., 1991).

Fluorescence Measurements. Fluorescence spectra were determined using an SLM 8000C spectrofluorometer (SLM Aminco, Urbana, IL). For rapid kinetics measurements, a Model !SX17MV stopped-flow spectrophotometer (Applied Photophysics Ltd., Leatherhead, U.K.) fitted with a 150 W Xe arc lamp was used with excitation at 290 nm (0.1−2 mm slits). Fluorescence emission from Trp residues was observed through a Corion 51660 (UG-1) band pass filter, while sensitized mant nucleotide fluorescence was observed through a Corion 51280 cuton filter. The UG-1 filter was used in the high-sensitivity port of the spectrophotometer. All reactions were performed at 4 °C, and the reported concentrations of reactants are those in the reaction chamber. The dead time of the !SX17MV instrument was determined to be 1.5 (±0.2) ms (Moore, 1992), and it had a mixing efficiency of >99% (Bagshaw et al., 1974). Typically, each trace shown is the average of 4−6 individual experiments, and the observed rate constants reported represent the mean and standard deviation of that data set. An instrumental time constant, which was maintained at <1% of the exponential half-time of the fastest reaction of interest, was used. Identical data were obtained using a KinTek SF-2001 stopped-flow instrument (KinTek Instruments, University Park, PA).

Kinetic Data Analysis. Stopped-flow kinetic time courses were analyzed using the nonlinear least-squares fitting routines supplied by Applied Photophysics. Kinetic simulation and analysis were performed with KSIM and KFIT (Dr. N. Millar, Kings College, London), while for the analysis of experimental data by computer simulation, the PC versions of KINSIM and FITSIM (from Dr. C. Frieden, this department) were used (Barshop et al., 1983; Zimmerle et al., 1987; Zimmerle & Frieden, 1989). The FITSIM analysis is described in more detail in the accompanying paper (Moore & Lohman, 1994). All programs were run on an IBM 486 PC. Rate and equilibrium constants reported in the text represent the resolved values and associated errors from fits of the data to eqs 1−4, accounting for the propagation of errors. Tables 1−3 report the mean values of the rate and equilibrium parameters determined from multiple experiments, along with an estimate of the range of values obtained in these studies.

RESULTS

We have observed that the steady-state rate of ATP hydrolysis by the Rep monomer (in the absence of added DNA) at 4 °C in buffer A varied from 0.003 to 0.011 s^{-1} (0.002−0.006 s^{-1} for mantATP hydrolysis) among different Rep preparations. However, the ss-DNA-stimulated ATPase activity of each preparation (assayed with poly(dT)) is invariant (within 10%) among these same preparations (Lohman et al., 1989). The variability in the DNA-independent ATPase activities most likely reflects the presence of low, but variable, amounts of contaminating DNA in each Rep preparation (see below). Assuming that this ATPase activity is comparable to that measured in the presence of dT_{16}, we estimate that <0.1% of the Rep protein used in these experiments is bound to DNA (K.J.M.M., unpublished results). The intrinsic hydrolysis of mantATP by Rep does not influence the predicted time courses of the fluorescence changes described here and is neglected in our analysis of the data. However, we note that this ATPase activity precludes the study of mantATP binding to Rep by equilibrium titration methods.

Fluorescence Changes Associated with mantATP Binding to Rep Monomer. The binding of ATP or ADP does not induce a significant change in the intrinsic tryptophan fluorescence of the Rep monomer. Therefore, we have used the fluorescent nucleotide analogue, 2′(3′)-*O*-(*N*-methylanthraniloyl)-ATP (mantATP, Figure 1A), to monitor nucleotide binding to the Rep monomer. The spectral properties of the mant fluorophore (Figure 1B) are ideally suited to monitor binding by changes in fluorescence resonance energy transfer (FRET) from Trp residues in Rep to the mant fluorophore bound at the ATP binding site. Figure 1C shows a stopped-flow recording when 5 μM mantATP is rapidly mixed with 0.2 μM Rep in buffer A at 4 °C. The 12% decrease in tryptophan fluorescence occurred exponentially with an observed rate constant (k_{obs}) of 59 (±0.6) s^{-1}. A 20-fold enhancement in the sensitized emission of the mant fluorophore (emission at >410 nm) also occurs upon binding to Rep (excitation = 290 nm) with k_{obs} = 61 (±0.2) s^{-1} (Figure 1C), which is consistent with the presence of FRET. Identical values of k_{obs} are determined by monitoring either protein or mant nucleotide fluorescence (see Figure 1C). In general, however, the enhancement of mant fluorescence has a significantly higher signal-to-noise ratio than the protein fluorescence signal and is routinely plotted in the figures presented here. The extremely low fluorescence intensity of mant nucleotides in solution at 290 nm, combined with the large fluorescence change, allows nucleotide binding to be monitored even in the presence of a large excess of nucleotide (e.g., see Figure 5B). Although a small increase

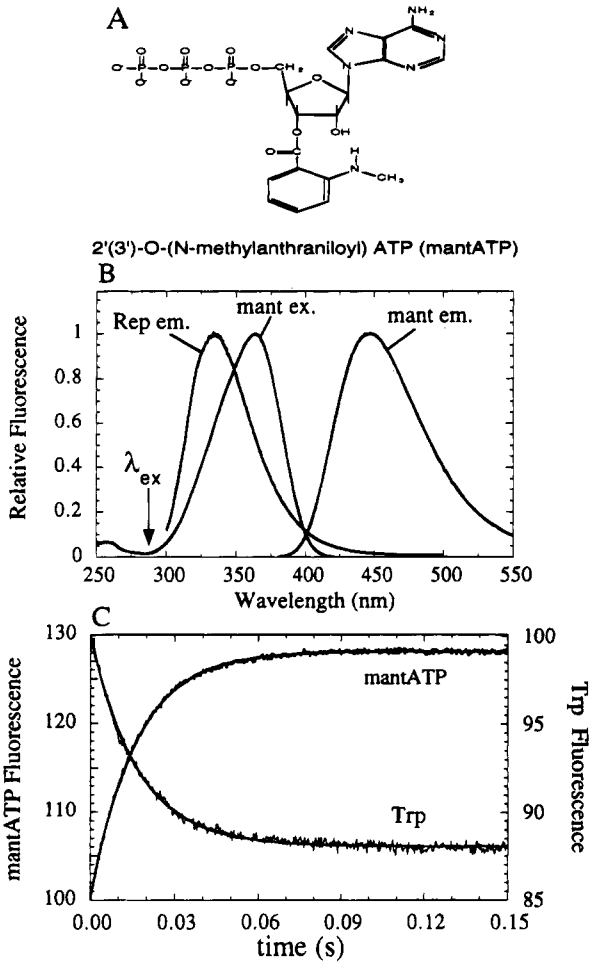

FIGURE 1: (A) Structure of 2′(3′)-*O*-(*N*-methylanthraniloyl)-ATP (mantATP). The 2′ and 3′ isomers of mant nucleotides exist as an equilibrium mixture (60% 3′ isomer) in slow exchange ($t_{1/2}$ = 10 min at pH 7.5, 25 °C). (B) Fluorescence overlap between the Rep monomer emission spectrum and the mant nucleotide excitation spectrum (λ_{ex} = 290 nm). (C) Change in fluorescence intensity (λ_{ex} = 290 nm, $\lambda_{em,Trp}$ = 300−400 nm, $\lambda_{em,mant}$ > 400 nm) when 0.2 μM Rep monomer in buffer A at 4 °C was rapidly mixed with 5 μM mantATP in the same buffer (reaction chamber concentrations). Solid lines represent the best fit of the data to a single exponential: (i) mantATP, k_{obs} = 61 s^{-1}, A = 29%; (ii) Trp, k_{obs} = 59 s^{-1}, A = 12%.

in mant nucleotide fluorescence (~20%) is observed upon binding Rep when the mant fluorophore is excited directly at 364 nm, the high background fluorescence of the mant nucleotides at this wavelength limits the concentration range over which nucleotide binding can be observed. We have therefore used an excitation wavelength of 290 nm to monitor the kinetics of mant nucleotide binding in these studies.

Biphasic Kinetics of mantATP Binding to Rep Monomer. The kinetics of mantATP binding to Rep at [mantATP] < 5 μM clearly is biphasic and requires the sum of two exponentials to describe the time course adequately. Figure 2A shows the increase in mant nucleotide fluorescence when 2 μM mantATP is mixed with 0.2 μM Rep. A fast phase, with observed rate constant $k_{obs,1}$ = 24 s^{-1} and amplitude A_1 ~ 0.85, was followed by a slower phase ($k_{obs,2}$ = 2.8 s^{-1}, A_2 ~ 0.15). Over the [mantATP] range of 1−15 μM, $k_{obs,1}$ varies linearly with [mantATP], yielding an apparent bimolecular association rate constant of (1.1 ± 0.02) × 10^7 M^{-1} s^{-1} and an intercept of 5.9 (±1.3) s^{-1} (Figure 2B). The amplitude of the slow phase decreases at higher concentrations of mantATP, becoming negligible above 5 μM.

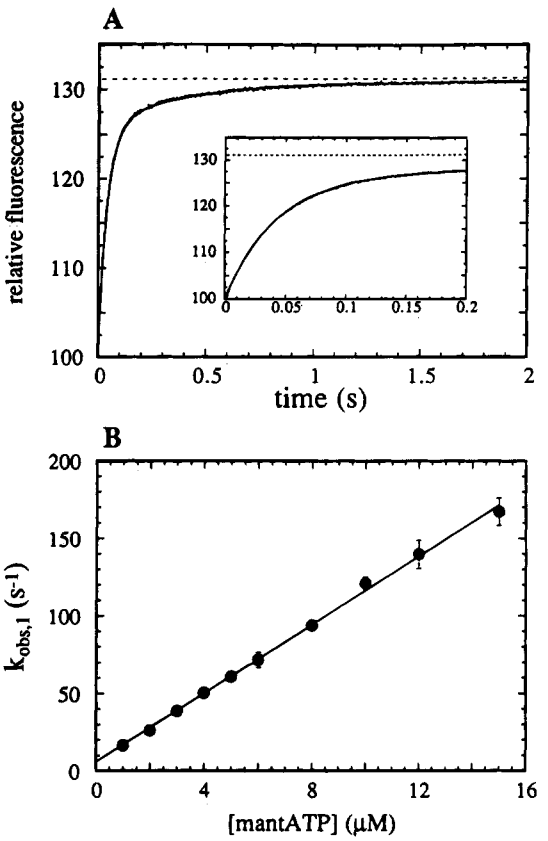

FIGURE 2: Kinetics of mantATP binding to 0.2 μM Rep monomer. (A) 0.2 μM Rep monomer in buffer A at 4 °C was rapidly mixed with 2 μM mantATP in the same buffer, and the increase in mantATP fluorescence was monitored with time. The solid line (superimposed) is a best fit of the data to the sum of two exponentials, with $k_{obs,1}$ = 24 s^{-1}, $k_{obs,2}$ = 2.8 s^{-1}, A_1 = 26%, and A_2 = 5%. Inset: As in A, except the reactions were monitored over 200 ms. (B) Dependence of $k_{obs,1}$ on [mantATP] from experiments such as those in A. Above 4 μM mantATP, the data were fit to a single exponential (see Figure 1C). The best fit of the data to a line yields a gradient = 1.1 × 10^7 M^{-1} s^{-1} and an intercept = 5.9 s^{-1}.

Similar experiments at a final Rep concentration of 30 nM were performed to define the [mantATP] dependence of the slow phase, while maintaining pseudo-first-order conditions (Figure 3A,B). A biphasic fluorescence increase was observed that was well described by the sum of two exponentials, although the amplitude of the fast process became too small to measure accurately below 10 nM mantATP. The total amplitude of the fluorescence change ($A_1 + A_2$) as a function of [mantATP] can be used to estimate the overall equilibrium constant for mantATP binding to Rep. A fit of this data to a 1:1 isotherm yields a value of $K_{overall}$ = 170 (±30) μM^{-1} (Figure 3B). The rate constant of the fast phase ([mantATP] ≥ 90 nM) increased linearly with [mantATP] [k_{+1} = (1.4 ± 0.2) × 10^7 M^{-1} s^{-1}) with an intercept of 6.1 (±0.2) s^{-1}, data not shown], in agreement with the data in Figure 2B obtained at 0.2 μM Rep. The rate constant for the slow phase, $k_{obs,2}$, showed a hyperbolic dependence on [mantATP], with a plateau at 2.9 (±0.05) s^{-1} and an intercept of ≪0.2 s^{-1} (Figure 4A).

The data presented in Figures 2−4 indicate that the association of mantATP with Rep monomer is more complex than a simple bimolecular association reaction. The simplest

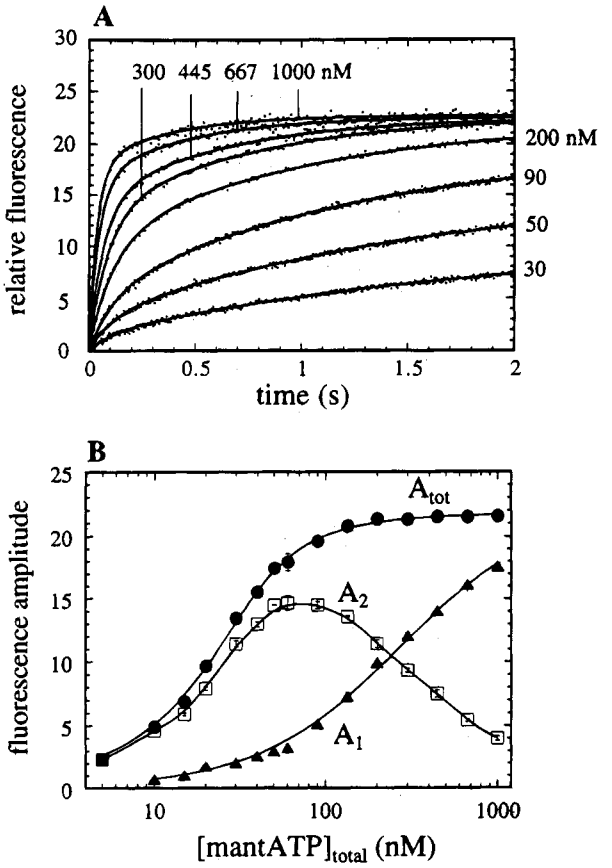

FIGURE 3: Kinetics of mantATP binding to 30 nM Rep monomer. (A) 30 nM Rep monomer in buffer A at 4 °C was rapidly mixed with 2−1000 nM mantATP. Representative traces are shown from 30 to 1000 nM mantATP. Each reaction was monitored for >6 half-times of the slowest phase, and the data are plotted on this scale for clarity. The solid lines represent the best fit of each curve to the sum of two exponentials. (B) Dependence of the exponential amplitudes of the fast and slow phases from the data in A on the total concentration of mantATP. Below 10 nM mantATP, the amplitude of the fast phase was too small to measure accurately. The solid lines for A_{tot} and A_1 are best fits of the data to Langmuir isotherms, with apparent association constants of 167 (±33) and 3.7 (±0.4) μM^{-1}, respectively. The data for A_2 are connected by a smooth line, which extrapolates to zero at [mantATP] > 5 μM.

Scheme 1

$$P + \text{mantATP} \underset{k_{-1}}{\overset{k_{+1}}{\rightleftharpoons}} \text{P–mantATP} \underset{k_{-2}}{\overset{k_{+2}}{\rightleftharpoons}} \text{(P–mantATP)*}$$

interpretation of these results is that nucleotide binding occurs in two sequential steps, as depicted in Scheme 1, where P represents the Rep monomer (for alternative interpretations, see the Discussion). On the basis of the observation that A_2 decreases to zero as [mantATP] increases (Figure 3B), we infer that the fluorescence intensities of P−mantATP and (P−mantATP)* are identical, and thus the observed fluorescence enhancement reflects the sum of the concentrations of these two species ([P−mantATP] + [(P−mantATP)*]). The values of the four rate constants in Scheme 1 were obtained as will be described here and are summarized in Table 1. The equilibrium association constants for each step in Scheme 1 are K_1 ($=k_{+1}/k_{-1}$) and K_2 ($=k_{+2}/k_{-2}$).

The fast phase of the fluorescence change reflects the binding of mantATP to P, while the slow phase reflects an isomerization of the P−mantATP complex. Under conditions that are pseudo-first-order in mantATP, and applying the square root approximation, the dependencies of $k_{obs,1}$ and

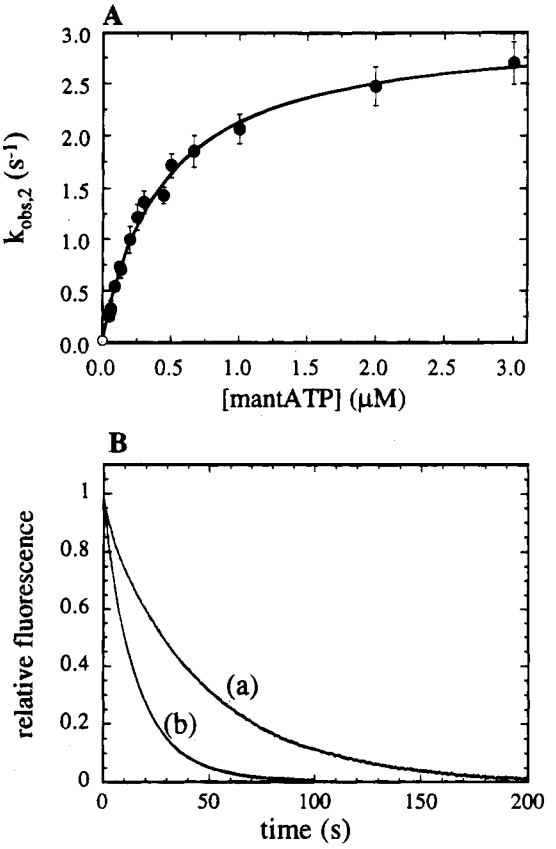

FIGURE 4: Dependence of $k_{obs,2}$ on [mantATP]. (A) Dependence of the observed rate constant of the slow phase ($k_{obs,2}$) from the data in Figure 3A on [mantATP] > 0.06 μM (●). The solid line is the best fit of the data to a simple hyperbola, with a plateau = 2.9 (±0.05) s^{-1} and K_{app} = 2.5 (±0.4) μM^{-1}. The intercept was fixed at 0.02 s^{-1} (○, see B). (B) Curve a: 0.2 μM Rep monomer in buffer A containing 3 μM mantATP was rapidly mixed at 4 °C with 1 mM ATP in the same buffer. The solid line is the best fit of the data to a single-exponential decay: k_{obs} = 0.021 s^{-1}. Curve b: Same as curve a, except that the Rep−mantATP complex was in buffer A + 50 μM $MgCl_2$ and the 1 mM ATP chase was in buffer AE + 10 mM EDTA (k_{obs} = 0.055 s^{-1}).

$k_{obs,2}$ are given by eqs 1 and 2, respectively (Johnson, 1992; Bernasconi, 1976):

$$k_{obs,1} \approx k_{+1}[\text{mantATP}] + k_{-1} + k_{+2} + k_{-2} \quad (1)$$

$$k_{obs,2} \approx \frac{k_{+1}[\text{mantATP}](k_{-2} + k_{+2}) + k_{-1}k_{-2}}{k_{+1}[\text{mantATP}] + k_{-1} + k_{+2} + k_{-2}} \quad (2)$$

Analysis of Figure 2B according to eq 1 yields k_{+1} = (1.1 ± 0.02) × 10^7 M^{-1} s^{-1} and $k_{-1} + k_{+2} + k_{-2}$ = 6 (±0.2) s^{-1}. According to eq 2, the plateau value for $k_{obs,2}$ at high [mantATP] (2.9 (±0.05) s^{-1}) equals $k_{+2} + k_{-2}$, and therefore we can calculate k_{-1} = 3.1 (±0.2) s^{-1}. The intercept of Figure 4A defines the *net* dissociation rate (k_{off}) of mantATP from the (P−mantATP)* complex and is related to the elementary rate constants in Scheme 1 by

$$k_{off} = \frac{k_{-2}k_{-1}}{k_{-1} + k_{+2} + k_{-2}} \quad (3)$$

The value of k_{off} was determined independently from a cold chase displacement experiment in which a preformed Rep−mantATP complex in buffer A (0.2 μM Rep, 3 μM mantATP) was mixed with 1 mM ATP (to prevent rebinding

Table 1: Rate and Equilibrium Constants for the Interaction of the Rep Monomer with mantNucleotides at 4 °C[a]

$$P + A \underset{k_{-1}}{\overset{k_{+1}}{\leftrightarrow}} P{-}A \underset{k_{-2}}{\overset{k_{+2}}{\leftrightarrow}} (PA)^*$$

nucleotide	k_{+1} (μM^{-1} s^{-1})	k_{-1} (s^{-1})	K_1 (μM^{-1})	k_{+2} (s^{-1})	k_{-2} (s^{-1})	K_2	k_{off} (s^{-1})	$K_{overall}$ (μM^{-1})	$K_{a,app}$[c] (calcd) (μM^{-1})	$k_{a,app}$[d] (obs) (μM^{-1})
mantATP	11 (±2)	3.2 (±0.5)	3.4 (±0.8)	2.9 (±0.2)	0.04 (±0.005)	73 (±10)	0.021 (±0.002)	228 (±62)	231 (±62)	167 (±23)
mantATP[b] ($-Mg^{2+}$)	80 (±10)	240 (±24)	0.33 (±0.05)	32 (±2)	38 (±3)	0.84 (±0.07)	29 (±2)	0.28 (±0.05)	0.61 (±0.07)	0.53 (±0.06)
mantATPγS	20 (±2)	11 (±3)	1.8 (±0.38)	19 (±3)	0.69 (±0.07)	28 (±0.99)	0.23 (±0.02)	51 (±2)	53 (±2)	>40
mantAMPPNP	0.66[e] (±0.04)	ND	0.015 (±0.002)	41 (±2)	0.61 (±0.05)	67 (±6)	0.61 (±0.05)	1.0 (±0.16)	1.0 (±0.16)	1.0 (±0.06)

[a] Conditions: 20 mM Tris·HCl (pH 7.5 at 4 °C), 6 mM NaCl, 5 mM $MgCl_2$, and 10% (v/v) glycerol (buffer A). [b] Conditions: 20 mM Tris·HCl (pH 7.5 at 4 °C), 6 mM NaCl, 2 mM EDTA, and 10% (v/v) glycerol (buffer AE). $K_{overall} = K_1K_2$. [c] Apparent overall affinity = $K_1 + K_1K_2$, calculated from estimates of K_1 and K_2. [d] Apparent overall affinity determined from fits of ΔF_{total} on [nucleotide] to a Langmuir isotherm. [e] Apparent association rate constant for mantAMPPNP = K_1k_{+2}. k_{off} is the observed rate of nucleotide dissociation from a Rep−nucleotide complex (see eq 3). $K_1 = k_{+1}/k_{-1}$; $K_2 = k_{+2}/k_{-2}$. ND:k_{-1} cannot be determined from these experiments, but is likely to be ≈700 s^{-1} [see Moore and Lohman (1994), accompanying paper].

of mantATP after dissociation). The majority of the fluorescence amplitude could be described by a single-exponential decay [curve a in Figure 4B; k_{obs} = 0.021 (±0.001) s^{-1}], which was independent of [ATP] from 0.2 to 1 mM. In addition, there was evidence of a faster process occurring at ~5 s^{-1} and comprising 1−2% of the total fluorescence change, which we attribute to the dissociation of mantATP from the small fraction of Rep in the P−mantATP complex. Simulation of the mechanism shown in Scheme 1 predicts such a process occurring at 5.2 s^{-1}. On the basis of the results of this experiment, the intercept in Figure 4A was fixed at 0.021 s^{-1}. From eq 3, and a knowledge of k_{off}, k_{-1}, and ($k_{-1} + k_{+2} + k_{-2}$), we calculate k_{+2} = 2.86 (±0.2) s^{-1} and k_{-2} = 0.04 (±0.005) s^{-1}.

We have also analyzed the kinetics of mantATP binding by numerical integration of the data using the program FITSIM (Zimmerle & Frieden, 1987; Barshop et al., 1983), which makes no simplifying assumptions and uses both the rate and amplitude dependence of the fluorescence changes [see Johnson (1992)]. The same rate constants (to within 10%) are obtained by using either the analytical approximation (eqs 1−3) or FITSIM. The fluorescence time courses over a wide range of [mantATP] could be described by kinetic simulation of Scheme 1 using the rate constants in Table 1 [see also Moore and Lohman (1994), accompanying paper]. These data are therefore consistent with a mechanism in which the initial binding of mantATP ($K_1 \sim 3.5\ \mu M^{-1}$) is followed by a first-order process ($K_2 \sim 70$), which may be a protein conformational change, leading to overall tight binding of mantATP ($K_{overall} = K_1K_2 \sim 200\ \mu M^{-1}$). The initial binding step does not appear to be rapidly reversible since $k_{-1} \sim k_{+2}$.

Kinetics of mantATPγS and mantAMPPNP Binding to the Rep Monomer. We have investigated the interaction of Rep with the mant derivatives of AMPPNP and ATPγS to determine their suitability as analogues of ATP in future kinetic studies of the Rep ATPase. The biphasic fluorescence change observed upon mixing 1 μM mantATPγS with 0.2 μM Rep (Figure 5A) is similar to that observed with mantATP. The exponential rates of the two phases, $k_{obs,1}$ and $k_{obs,2}$, increased with [mantATPγS] linearly and hyperbolically, respectively (data not shown). In order to extract elementary rate constants, we used the analysis described by Bernasconi (1976) since the square root approximation is not valid for mantATPγS. From knowledge of k_{off} = 0.23 (±0.01) s^{-1}, determined from a cold chase displacement experiment, we obtain the rate constants shown in Table 1, which are consistent with the [mantATPγS] dependence of the fluorescence amplitudes. All four rate constants for mantATPγS are faster than those for mantATP, most notably the two reverse rate constants. However, the equilibrium constants K_1 and $K_{overall}$ are not dissimilar from those obtained with mantATP (Table 1).

The binding of mantAMPPNP to Rep is (macroscopically) slow compared with either mantATP or mantATPγS and is characterized by only a single-exponential increase in nucleotide fluorescence (Figure 5B) over a wide range of [mantAMPPNP] (0.05−160 μM) and times (0.1−500 s). The observed rate constant, k_{obs}, increases hyperbolically with [mantAMPPNP] (Figure 5B, inset; Table 1), while the total amplitude of the fluorescence change (0.2 μM Rep, 0.05−100 μM mantAMPPNP) could be fit to a 1:1 binding isotherm with $K_{overall} = 0.98\ \mu M^{-1}$, which is nearly identical to the value obtained from an equilibrium fluorescence titration (1.1 μM^{-1}). In a cold chase displacement experiment with a Rep−mantAMPPNP complex, the majority of the fluorescence change (>90%) occurred with a rate constant of 0.61 (±0.02) s^{-1} (data not shown), which provides a more accurate estimate of the intercept in Figure 5B (inset). The simplest interpretation of these data is the two-step mechanism shown in Scheme 1, where the initial binding step is assumed to be rapidly reversible [see Moore and Lohman (1994), accompanying paper], and the rate and equilibrium constants shown in Table 1 were determined using this model. We have observed no curvature in plots of k_{obs} *vs* [mantATP] up to ~400 s^{-1} (the fastest rate measured).

These data suggest that any steps subsequent to the fluorescence change observed in the transient kinetic experiments do not produce a measurable increase in the overall

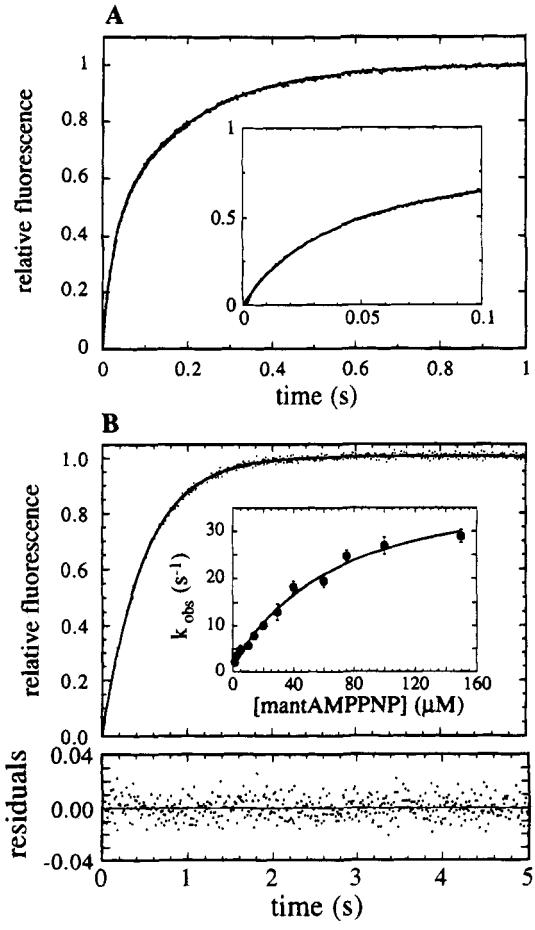

FIGURE 5: Kinetics of mantATPγS and mantAMPPNP binding to the Rep monomer. (A) 0.2 μM Rep monomer in buffer A at 4 °C was rapidly mixed with 1 μM mantATPγS. The solid line is a best fit of the data to the sum of two exponentials, with $k_{obs,1} = 43$ s^{-1}, $k_{obs,2} = 5.2$ s^{-1}, and $A_1/A_2 = 0.7$. Inset: As for A, except the reaction was monitored over 100 ms. (B) As for A, except 1 μM mantATPγS was replaced with 1 μM mantAMPPNP. The solid line is the best fit of the data to a single exponential, with $k_{obs} = 2.0$ s^{-1}. The deviation of the data from the best fit is shown in the bottom panel. Inset: Dependence of k_{obs} from experiments such as those in B on [mantAMPPNP]. The solid line is the best fit to a hyperbola, with a plateau = 42 s^{-1}, $K_{app} = 0.016$ (±0.001) μM^{-1}, and intercept = 1.3 s^{-1}.

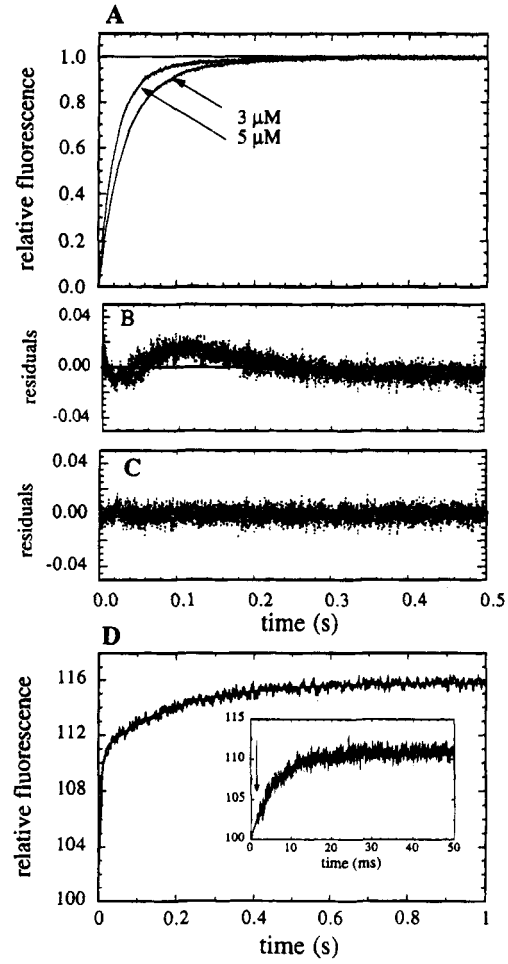

FIGURE 6: Binding of 3′-mant-dATP and mantADP to the Rep monomer. (A) 0.2 μM Rep monomer in buffer A at 4 °C was rapidly mixed with 3 or 5 μM 3′-mant-dATP as indicated. The solid lines (superimposed) are the best fits of each trace to the sum of two exponentials as follows: (i) 3 μM 3′-mant-dATP, $k_{obs,1} = 33$ s^{-1}, $k_{obs,2} = 10.5$ s^{-1}, $A_1 = 0.85$, $A_2 = 0.15$; (ii) 5 μM 3′-mant-dATP, $k_{obs,1} = 49$ s^{-1}, $k_{obs,2} = 11.3$ s^{-1}, $A_1 = 0.94$, $A_2 = 0.06$. (B and C) Deviations of the experimental data from the best fit to single- (B) and double- (C) exponential functions. Residuals from both the 3 and 5 μM data are superimposed. (D) 0.2 μM Rep monomer in buffer A at 4 °C was rapidly mixed with 4 μM mantADP. The solid line is the best fit of the data to the sum of two exponentials, where $k_{obs,1} = 148$ s^{-1}, $k_{obs,2} = 5.1$ s^{-1}, $A_1 = 11\%$, $A_2 = 5\%$. Inset: As for D, except the reaction was monitored over 50 ms. The arrow indicates the time at which flow stopped.

binding affinity. However, in the cold chase displacement experiment, there was clear evidence for a slower phase occurring at ~0.05 s^{-1} with <10% of the signal, which may represent the dissociation of mantAMPPNP from a more tightly bound complex present at low concentrations. Kinetic studies of AMPPNP binding to the Rep monomer (Moore & Lohman, 1994) provide direct evidence for such an additional species.

Binding of mant Deoxyribonucleotides to the Rep Monomer. It is well documented that mant nucleotides exist in solution as an equilibrium mixture of both the 2′ and 3′ isomers, which are in slow base-catalyzed exchange ($t_{1/2}$ ~ 10 min, pH 7.5, 25 °C) (Cremo et al., 1990; Eccleston et al., 1991; Woodward et al., 1991; Moore et al., 1993; Rensland et al., 1991; Moore, 1992). The two isomers can be separated by reverse phase HPLC (Moore et al., 1993) and are present in approximately equal concentrations (60% 3′ isomer). The 3′ isomers of mant nucleotides have twice the fluorescence intensity (Eccleston et al., 1991; Moore et al., 1993; Rensland et al., 1991) of the 2′ isomers, and this difference is directly reflected in their fluorescence lifetimes (Moore, 1992). Since acyl migration potentially may be responsible for either of the fluorescence changes observed here, we investigated the interaction of Rep with two additional classes of mant nucleotides, where the fluorophore is specifically attached to one (3′-mant-2′-deoxy) or two (2′,3′-bismant) sites on the ribose sugar. In both cases, acyl migration and preferential isomer binding cannot occur, and thus any biphasicity that is observed with these nucleotides must reflect an intrinsic property of the Rep−nucleotide complex.

The kinetics of 3′-mant-dATP binding to Rep are qualitatively similar to those observed with 2′(3′)-mantATP, although the biphasicity in the time course of 3′-mant-dATP binding to Rep was less pronounced than that observed with mantATP. The sum of two exponentials is required to describe the reaction of 3 and 5 μM 3′-mant-dATP with 0.2 μM Rep (Figure 6A−C). However, only the time courses

determined at 3′-mant-dATP concentrations between ~2 and 5 μM could be resolved into the sum of two exponentials; above 5 μM, the amplitude of the second phase became <5% of the total amplitude (although $k_{obs,2}$ appeared to plateau at ~12 s^{-1}), while below 2 μM 3′-mant-dATP, the rates and amplitudes of the two phases became too similar to resolve with confidence. The concentration dependence of the total amplitude yields an apparent equilibrium constant $K_{overall}$ = 1.8 (±0.2) μM^{-1}, compared to ~200 μM^{-1} with mantATP. The time course of dissociation of 3′-mant-dATP from a Rep−3′-mant-dATP complex is characterized by a double-exponential process ($k_{obs,1}$ = 4.5 s^{-1}, $k_{obs,2}$ = 0.2 s^{-1}, A_1/A_2 ~ 10), consistent with the presence of a small fraction of (P−3′-mant-dATP)* at equilibrium. Therefore, the binding of Rep monomer to both mantATP and 3′-mant-dATP requires a minimum of a two-step binding reaction (see later), as does the binding of nucleotides without the fluorescent modification (Moore & Lohman, 1994).

We have also investigated the interaction of Rep with bismant nucleotide derivatives, which contain a fluorophore on both hydroxyl residues. The fluorescence change following the reaction of Rep with both bismantATP and bismantATPγS is clearly biphasic over a range of nucleotide concentrations with observed rate constants similar to those observed with isomeric mixtures (data not shown). We therefore conclude that the biphasic time courses observed in these kinetics experiments are unrelated to acyl migration of the fluorophore or preferential isomer binding. Finally, we note that both isomers of mantATP are hydrolyzed by Rep in the presence of ss-DNA at comparable rates (K.J.M.M., unpublished data).

Kinetics of mantADP Binding to the Rep Monomer. The binding of mantADP to Rep is also associated with a biphasic fluorescence change (Figure 6D). The pseudo-first-order rate constant of the fast phase increases linearly with [mantADP] [k_{+1} = (7.1 ± 0.2) × 10^6 M^{-1} s^{-1}, intercept = 106 (±7) s^{-1}, K_1 = 0.071 (±0.011) μM^{-1}]. The amplitude of the fast phase increases with [mantADP] over the range 1−15 μM, consistent with the weaker initial binding of mantADP *vs* mantATP. The rate of the slow phase increases with increasing [mantADP] and is comparable to that observed with mantATP under similar conditions. We have not characterized the slow phase of the fluorescence change quantitatively due to its small amplitude and the fast rate of the first process. Nevertheless, these data suggest that Scheme 1 can also describe the kinetics of mantADP binding, which is consistent with our conclusions based on kinetic studies of ADP binding (Moore & Lohman, 1994). Consistent with the presence of a tightly bound Rep−mantADP complex, the dissociation of mantADP is characterized by at least two exponential processes occurring with observed rate constants of $k_{off,1}$ = 100 (±10) s^{-1} and $k_{off,2}$ = 0.45 (±0.03) s^{-1}. The slow phase of the fluorescence change presumably represents the dissociation of mantADP from a (P−mantADP)* complex. Similar results are obtained with 3′-mant-dADP [k_{+1} = (7.2 ± 0.3) × 10^6 M^{-1} s^{-1}, intercept = 70 (±5) s^{-1}, $k_{off,1}$ = 60 (±5) s^{-1}, $k_{off,2}$ = 1.2 (±0.1) s^{-1}].

Temperature Dependence of mantATP Binding to the Rep Monomer. The experiments described earlier were performed at 4 °C mainly to enable comparisons with our previous Rep−DNA binding studies, which were also performed at 4 °C. We have, however, examined the temperature dependence of the kinetics of 3′-mant-dATP and

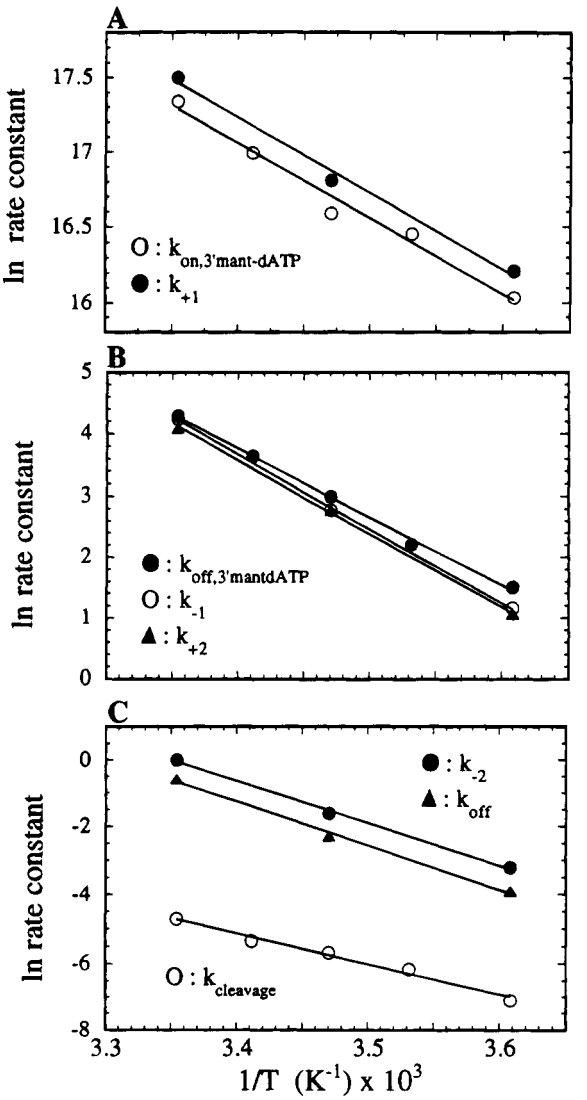

FIGURE 7: Temperature dependence of mantATP and 3′-mant-dATP binding to the Rep monomer. (A) Arrhenius plots of the apparent association rate constant, k_{on}, for 3′-mantATP (●) and of the bimolecular association rate constant, k_{+1}, for mantATP (○). (B and C) Arrhenius plots of the first-order rate constants from Scheme 1. (B) (●) k_{off} for 3′-mant-dATP; (○) k_{-1} for mantATP; (■) k_{+2} for mantATP. (C) (●) k_{-2} for mantATP; (▲) k_{off} for mantATP; (○) mantATP cleavage rate constant (Table 3).

mantATP binding from 4 to 25 °C (Figure 7, Table 2), since duplex DNA unwinding studies generally have been performed at higher temperatures (Amaratunga & Lohman, 1993). At higher temperatures, the binding of both nucleotides to Rep is faster, although weaker, while the maximal fluorescence amplitudes decrease.

With mantATP, estimates of all four rate constants could be obtained at 15 and 25 °C, although at 25 °C the uncertainties in the individual rate constants increase to ~25%. All four rate constants for mantATP binding to Rep, in addition to the net dissociation rate constant (k_{off}), increase with increasing temperature (Figure 7, Table 2). The equilibrium constant for the first step, K_1, decreases with increasing temperature, which is consistent with the [mantATP] dependence of the fluorescence amplitudes at higher temperatures. The equilibrium constant for the second step, K_2 (70 ± 10), does not appear to be sensitive to temperature. The reduction in the overall equilibrium association constant

Table 2: Temperature Dependence of the Binding of mant Nucleotides to the Rep Monomer[a]

$$P + A \underset{k_{-1}}{\overset{k_{+1}}{\leftrightarrow}} PA \underset{k_{-2}}{\overset{k_{+2}}{\leftrightarrow}} (PA)^*$$

temperature (°C)	k_{+1} ($\times 10^7$) (M^{-1} s^{-1})	k_{-1} (s^{-1})	k_{+2} (s^{-1})	k_{-2} (s^{-1})	k_{off} (s^{-1})	K_1 (μM^{-1})	K_2	K_1K_2 (μM^{-1})
4	1.1	3.2	2.9	0.04	0.02	3.4	73	230
	(0.92)[b]	(4.5)						(2.04)
10	(1.4)	(9.1)						(1.50)
15	2.0	16	16	0.20	0.10	1.3	80	100
	(1.6)	(20)						(0.82)
20	(2.4)	(38)						(0.62)
25[c]	≈4	≈70	≈60	≈1	0.56	≈0.5	≈60	≈30
	(3.4)	(73)						(0.46)

[a] Conditions: 20 mM Tris·HCl (pH 7.5 at the indicated temperature), 6 mM NaCl, 5 mM $MgCl_2$, and 10% (v/v) glycerol (buffer A). [b] Data in parentheses are for 3′-mant-dATP. All other data are for 2′(3′)-mantATP. [c] Data at 25 °C are subject to larger error (≈25%) than those at 4 and 15 °C, but are consistent with the [mantATP] dependence of the fluorescence amplitudes, A_1, A_2, and A_{total}.

($K_{overall} = K_1K_2$) with increasing temperature therefore reflects changes primarily in K_1.

The kinetic time courses for 3′-mant-dATP binding were generally of insufficient quality to extract two rate constants with confidence and therefore were fit to a single-exponential function. Thus, for 3′-mant-dATP all four rate constants could not be resolved, and we report only the apparent association and dissociation rate constants, k_{on} and k_{off}. With 3′-mant-dATP, both k_{on} and k_{off} increase with increasing temperature (Figure 7, Table 2), as determined from the slopes and intercepts, respectively, of plots of k_{obs} *vs* [3′-mant-dATP]. The intercept value is essentially identical within experimental error to the dissociation rate constant measured from a cold chase displacement experiment with excess ATP. The apparent equilibrium constant, K_{app} ($=k_{on}/k_{off}$) decreases ~5-fold from 4 to 25 °C, indicating that $\Delta H° < 0$. The apparent activation energies for the association and dissociation steps with 3′-mant-dATP are +10.0 (±0.6) and +18.9 (±1.8) kcal mol^{-1}, respectively (Figure 7A, Table 2). The limited size of the data set with mantATP precludes an accurate estimation of the activation energies for the individual steps in the binding mechanism. However, the association and dissociation rate constants observed with mantATP are comparable to those observed with 3′-mant-dATP at the same temperature (Table 2).

Effects of Mg^{2+} on mantATP Binding to the Rep Monomer. All of the experiments described above were performed in the presence of 5 mM $MgCl_2$. Using a protease digestion assay, Chao and Lohman (1990) reported evidence that ATP can bind to Rep in the absence of Mg^{2+}; however, Mg^{2+} is required to detect ATP binding to Rep by nitrocellulose filter binding (Arai et al., 1981a). To investigate this apparent discrepancy, we examined the effects of Mg^{2+} concentration on the kinetics of nucleotide binding to the Rep monomer. Mg^{2+} binding to Rep could not be monitored directly since the binding of Mg^{2+} does not change the intrinsic tryptophan fluorescence of Rep.

We initially performed experiments to determine whether mantATP could bind to Rep in the absence of Mg^{2+}. These experiments were performed in buffer AE, *without* added Mg^{2+}, and in the presence of 2 mM EDTA. A biphasic increase in mant nucleotide fluorescence was observed when 0.2 μM Rep (in buffer AE) was mixed with 2 μM mantATP in the same buffer (Figure 8A). The exponential rate constants of both phases ($k_{obs,1}$ = 450 s^{-1}, $k_{obs,2}$ = 47 s^{-1}) were much faster than those observed in the presence of 5 mM $MgCl_2$ (buffer A, Figure 2A). Increasing the EDTA concentration to 20 mM had no further influence on the observed rate constants. The fluorescence change observed when excess (5 mM) $MgCl_2$ was added to the mantATP solution in Figure 8A was indistinguishable from that observed in Figure 2A (data not shown). These results indicate that mantATP can bind to Rep even in the absence of Mg^{2+} ($<10^{-10}$ M Mg^{2+}), thus ruling out the possibility that Rep binds mantATP only as the Mg^{2+}–mantATP complex. The following experiments provide estimates of the elementary rate constants for mantATP binding to the Rep monomer in the absence of Mg^{2+}.

Experiments analogous to those shown in Figure 8A were performed with a range of [mantATP] of 0.5–25 μM in buffer AE at 4 °C. The observed rate constant of the fast phase, $k_{obs,1}$, increased linearly with [mantATP] [k_{+1} = (8 ± 1) × 10^7 M^{-1} s^{-1}, intercept = 300 (±20) s^{-1}], while the total fluorescence amplitude increased hyperbolically with an apparent $K_{overall}$ = 0.53 (±0.05) μM^{-1}. The observed rate constant for the slow phase, $k_{obs,2}$, increased hyperbolically with [mantATP], as shown in Figure 8B, with an intercept = 29 (±2) s^{-1} and a plateau = 69 (±2) s^{-1} [K_{app} = 0.38 (±0.04) μM^{-1}]. Dissociation of mantATP from a Rep–mantATP complex (0.2 μM Rep + 10 μM mantATP) in the presence of 1 mM ATP (Figure 8C) displayed a biphasic decrease in fluorescence intensity [$k_{obs,1}$ = 240 (±24) s^{-1}, $k_{obs,2}$ = 29 (±0.5) s^{-1}]. We attribute the fast phase of this process to the dissociation of mantATP from P–mantATP ($k_{obs,1} \sim k_{-1}$), while the slow phase monitors the slower dissociation of mantATP from (P–mantATP)* ($k_{obs,2} = k_{off} \sim k_{-2}$). The observed rate constant of the slower process observed in Figure 8C (k_{off} = 29 s^{-1}) is in excellent agreement with the intercept of Figure 8B (29 s^{-1}), which should also define k_{off} (eq 3) under these conditions. Fitting the data in Figure 8 to Scheme 1 and eqs 1–3 yields estimates of all four rate constants for the binding of mantATP in the absence of Mg^{2+} (Table 1). All four rate constants are larger than those determined in the presence of excess (5 mM) Mg^{2+}. In the absence of Mg^{2+}, k_{-1} and k_{off} increase ~100-fold and ~1500-fold, respectively, indicating that Mg^{2+} has a major stabilizing influence on the

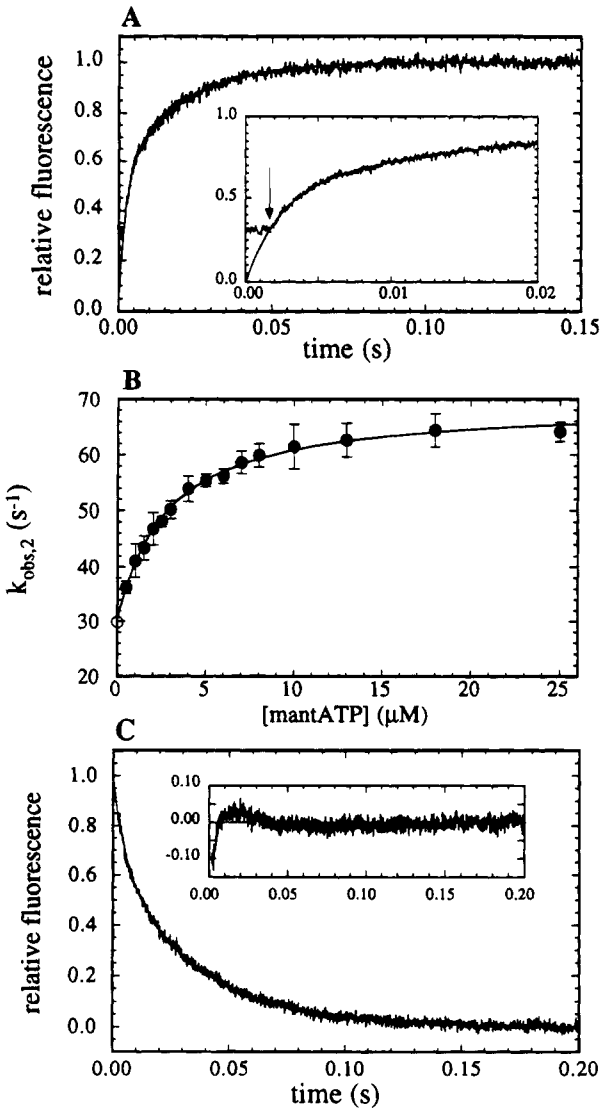

FIGURE 8: Kinetics of mantATP binding to the Rep monomer in the absence of Mg^{2+}. (A) 0.2 μM Rep monomer in buffer A minus $MgCl_2$ + 2 mM EDTA (buffer AE) was rapidly mixed with 2 μM mantATP in the same buffer at 4 °C. The solid line (superimposed) is the best fit of the data to the sum of two exponentials, where $k_{obs,1}$ = 454 s^{-1}, $k_{obs,2}$ = 47 s^{-1}, A_1/A_2 = 1.2. Inset: As for A, except the reaction was monitored over 20 ms. (B) Dependence of $k_{obs,2}$ from the experiments shown in A on [mantATP]. The solid line is the best fit to a hyperbola, with intercept = 29 s^{-1}, plateau = 69 s^{-1}, and K_{app} = 0.38 (±0.04) μM. (C) 0.2 μM Rep + 10 μM mantATP in buffer AE was rapidly mixed with 1 mM ATP in the same buffer at 4 °C. The solid line (superimposed) is the best fit to two exponentials, with $k_{obs,1}$ = 240 s^{-1}, $k_{obs,2}$ = 29 s^{-1}, and $A_1/A_2 \sim 0.5$. Inset: The residuals from a best fit of the data in C to a single-exponential decay.

formation of the P−mantATP and (P−mantATP)* complexes.

Kinetics of Mg^{2+} Dissociation from Rep−mantATP Complexes. The presence of Mg^{2+} greatly increases the kinetic and thermodynamic stability of the P−mantATP and (P−mantATP)* complexes, probably due to the formation of P−Mg^{2+}−mantATP and (P−Mg^{2+}−mantATP)* ternary complexes. Since both Mg^{2+} and free mantATP can bind to the Rep monomer independently (see preceding sections and Discussion), it was of interest to determine whether mantATP and Mg^{2+} can *dissociate* independently or whether nucleotides are relased from Rep only as their Mg^{2+} complexes (or both). These possibilities can be distinguished

Scheme 2

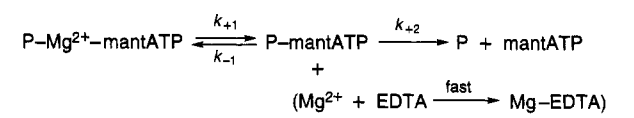

Scheme 3

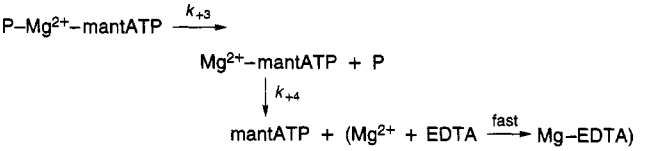

Scheme 4

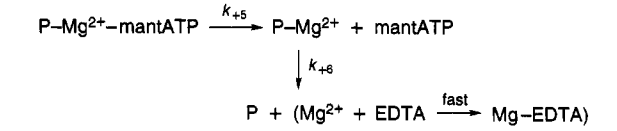

by monitoring the kinetics of mantATP dissociation from (P−Mg^{2+}−mantATP)* upon the addition of EDTA, which chelates the free Mg^{2+} [see Bagshaw and Trentham (1974), Eccleston (1981), and John et al. (1993)]. In the discussion that follows, we treat the kinetically important site for Mg^{2+} binding as the ATP binding site by analogy with other nucleotide binding proteins. However, we cannot exclude the possibility that Mg^{2+} binding to an additional separate site on the Rep monomer influences the kinetics of mantATP binding and dissociation.

Upon mixing a Rep−Mg^{2+}−mantATP complex with excess EDTA and ATP, the dissociation of mantATP and Mg^{2+} can, in principle, occur by any of the three mechanisms in Schemes 2−4. The observed rate of mantATP dissociation (k_{diss}) in the presence of excess ATP according to Schemes 2−4 is then given by

$$k_{diss} = [(k_{+1}k_{+2})/(k_{+1} + k_{-1}[Mg^{2+}] + k_{+2})] + k_{+3} + k_{+5} \quad (4)$$

Since $k_{+1} \ll k_{+2}$ (see below), eq 4 predicts that k_{diss} will decrease approximately hyperbolically from $k_{diss} = k_{+1} + k_{+3} + k_{+5}$ in the presence of excess EDTA to $k_{diss} = k_{+3} + k_{+5}$ in the presence of excess Mg^{2+}. The difference between these limiting values can be used to estimate k_{+1}, the rate constant for the independent dissociation of Mg^{2+} from the ternary complex (Scheme 2). When a Rep−mantATP complex in 50 μM $MgCl_2$ was mixed with 10 mM EDTA plus 1 mM ATP, k_{diss} was measured to be 0.055 (±0.003) s^{-1} (Figure 4B, curve b), compared to 0.021 (±0.002) s^{-1} in the presence of 5 mM $MgCl_2$ (Figure 4B, curve a). These limiting values were unaffected by increasing the [EDTA] or [Mg^{2+}]. The difference between these values yields k_{+1} = 0.034 (±0.004) s^{-1}, which indicates that both the nucleotide and the Mg^{2+} dissociate from the ternary complex at comparable rates. Similar values for k_{+1} were obtained with 3′-mant-dATP, mantAMPPNP, mantADP, and 3′-mant-dADP. However, a considerably higher value for k_{+1} was obtained with mantATPγS [k_{+1} = 0.22 (±0.01) s^{-1}].

DNA-Independent Single-Turnover Cleavage of mantATP and ATP by the Rep Monomer. Rep, along with other helicases, is often referred to as a DNA-dependent ATPase, although the true rate of ATP cleavage by DNA-free Rep has not been measured quantitatively. In fact, all previous

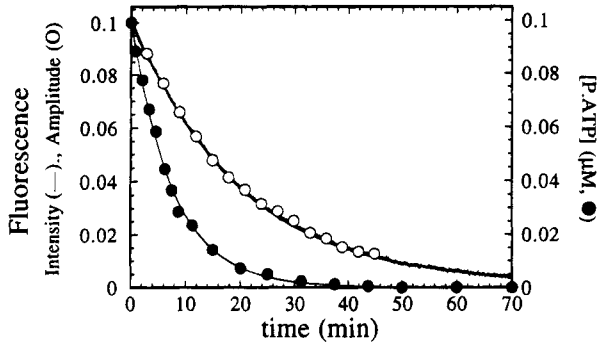

FIGURE 9: Single-turnover cleavage of mantATP by the Rep monomer. ●: 0.2 μM Rep monomer in buffer A at 4 °C was manually mixed with 0.1 μM [α-^{32}P]ATP in the same buffer. At the time points indicated, aliquots of the reaction were quenched into $HClO_4$ and analyzed for [α-^{32}P]ADP as described under Materials and Methods. The solid line is the best fit to an exponential decay in [P−ATP], where $k_{obs} = 2.1 \times 10^{-3}$ s^{-1}. Continuous data: 0.2 μM Rep (from two preparations) in buffer A at 4 °C was rapidly mixed with 0.1 μM mantATP. The slow decay in fluorescence (superimposed) could be described by a single-exponential decay for both protein preparations ($k_{obs} = 0.82 \times 10^{-3}$ s^{-1}). ○: 0.4 μM Rep + 0.2 μM mantATP in buffer A at 4 °C was incubated in the drive syringes of the stopped-flow apparatus. After various incubation times, a sample of the reaction mixture was rapidly mixed with 1 mM ATP. The amplitude of the observed fluorescence change in the chase experiment is plotted as a function of the incubation time. The solid line is the best fit of the data to a single-exponential decay ($k_{obs} = 0.80 \times 10^{-3}$ s^{-1}).

measurements of Rep ATPase activity (±DNA), as well as those of other helicases, have been steady-state measurements performed in excess ATP (Kornberg et al., 1978; Arai et al., 1981a; Wong et al., 1993), which can be greatly influenced even by very small amounts of contaminating DNA contained within the protein stocks.

The high affinity of the Rep monomer for mantATP and ATP (Moore & Lohman, 1994) suggested that the rate of nucleotide hydrolysis by DNA-free Rep monomer could be determined directly by monitoring a single-turnover reaction in the presence of excess Rep. Three approaches were used to obtain estimates of the true DNA-independent ATP and mantATP cleavage rates with the Rep monomer. The first approach measured the single-turnover rate of ATP cleavage using radiolabeled ATP. The cleavage of 0.1 μM [α-^{32}P]-ATP in the presence of 0.2 μM Rep (>90% ATP bound) at 4 °C is shown in Figure 9 and is described by a single-exponential decay with $k_{obs} = 2.1 \times 10^{-3}$ s^{-1}. Further experiments with a 5-fold excess of ATP (1 μM) showed no sign of a burst of product formation, suggesting that product release is not rate-limiting in this reaction.

A continuous fluorescence assay was used to measure the single-turnover rate of mantATP cleavage. Since mant-ADP binds weakly to Rep and product release is not rate-limiting, as discussed earlier (k_{off} for mantADP = 0.45 s^{-1}), the binding of 0.1 μM mantATP to 0.2 μM Rep (which results in >95% of the mantATP bound to Rep) will be followed by a decrease in mant nucleotide fluorescence intensity, which reflects the dissociation of mantADP but which is *limited* by the rate of mantATP hydrolysis. The time course of mantATP hydrolysis determined in this manner follows a single-exponential decay with $k_{obs} = 8.3 \times 10^{-4}$ s^{-1} (Figure 9, continuous data). We observe superimposable time courses for two such experiments performed with two preparations of Rep, which show a 4-fold difference in their *apparent* steady-state DNA-independent ATPase activities.

Table 3: Temperature Dependence of the First-Order mantATP Cleavage Rate Constant[a]

temperature (°C)	mantATP cleavage rate constant ($\times 10^{-3}$ s^{-1})
4	0.83 (±0.04)
10	2.1 (±0.05)
15	3.4 (±0.04)
20	4.8 (±0.06)
25	9.0 (±0.08)

[a] Conditions: 20 mM Tris·HCl (pH 7.5 at the indicated temperature), 6 mM NaCl, 5 mM $MgCl_2$, and 10% (v/v) glycerol (buffer A).

An independent estimate of the rate of mantATP cleavage was obtained using a different approach. The amplitude of the fluorescence change (ΔF_{obs}) observed in a cold chase mantATP displacement experiment (e.g., Figure 4B, curve a) is proportional to ([P−mantATP] + [P−mantATP)*]), which is dominated by the concentration of (P−mantATP)* (since $K_2 \gg 1$). Therefore, the rate of mantATP hydrolysis can also be determined by performing displacement experiments as a function of the incubation time. In the presence of excess Rep, ΔF_{obs} will decrease exponentially with incubation time at a rate that defines the first-order rate of mantATP cleavage. The results of this experiment are shown in Figure 9, from which we calculate $k_{obs} = 8.0 \times 10^{-4}$ s^{-1}. This rate constant is essentially identical to that obtained earlier using the continuous assay (8.3×10^{-4} s^{-1}).

We have measured the first-order rate of mantATP hydrolysis as a function of temperature (0.03 μM mantATP, 0.4 μM Rep), and the results are given in Table 3. The cleavage rate increases with increasing temperature, with an apparent activation energy of 18 (±2) kcal mol^{-1} for the cleavage step [Figure 7C, $k_{obs} = (9.0 \pm 0.1) \times 10^{-3}$ s^{-1} at 25 °C]. These studies indicate that the rate of mantATP hydrolysis is >25-fold slower than the slowest rate constant measured in Figures 1−8, and therefore mantATP hydrolysis does not interfere with the kinetic measurements for any of the hydrolyzable nucleotides studied here.

DISCUSSION

Application of Fluorescent Nucleotide Analogues. The experiments described here focus on the kinetic mechanism of mant nucleotide binding to the *E. coli* Rep monomer. The kinetics and mechanism of Rep binding to ATP, ADP, and other nonfluorescent ligands are discussed by Moore and Lohman [1994 (accompanying paper)]. These studies represent a basic characterization of the nucleotide binding properties of the Rep monomer, which provides the necessary background and the approaches for subsequent studies of the functionally active dimeric Rep helicase that forms upon binding DNA (Wong et al., 1992; Wong & Lohman, 1992).

mant nucleotides have been used successfully to investigate the kinetic mechanisms of a number of other ATPases (Hiratsuka, 1983; Cremo et al., 1990; Woodward et al., 1991; Sadhu & Taylor, 1992) and GTPases (Neal et al., 1990; Moore et al., 1993; Eccleston et al., 1991, 1993; Brownbridge et al., 1993; John et al., 1990). For our studies with Rep, mant nucleotides were found to be more useful than 2,4,6-trinitrophenyl-ATP (TNP-ATP) and 1,N^6-ethenoadenosine triphosphate (ϵATP). The 20-fold increase in sensitized fluorescence emission observed upon binding mantATP to

Rep allows the kinetics of nucleotide binding to be examined over a wide range of nucleotide concentrations. The use of sensitized emission is likely to be particularly useful in cases where the fluorescence intensity of the mant fluorophore itself is not significantly perturbed upon binding to the protein of interest. The observed fluorescence change occurs upon the association of mantATP to Rep (step 1 of Scheme 1), with P−mantATP and (P−mantATP)* possessing equal fluorescence intensities, indicating that the fluorescence change monitors only the difference between free and bound nucleotides. Since both phases of the binding reaction are observed, all four elementary rate constants can be determined either analytically or by numerical integration techniques (Barshop et al., 1983; Zimmerle & Frieden, 1989; Zimmerle et al., 1987), with identical results.

The kinetics of mant nucleotide binding to the Rep monomer are similar to those observed with the parent nucleotides (Moore & Lohman, 1994). Furthermore, both the Rep monomer (Figure 9) and dimeric Rep−DNA complexes (K.J.M.M., unpublished data) hydrolyze mantATP at rates that are comparable to those observed with ATP. Rep-catalyzed unwinding of duplex DNA is also efficiently supported by mantATP (K. P. Bjornson, K.J.M.M., and T.M.L., unpublished data), and thus mant nucleotides will be useful in future studies of the DNA unwinding mechanism of Rep and other helicases.

mant nucleotides exist as a mixture of 2′ and 3′ isomers that are present in approximately equal concentrations (Cremo et al., 1990; Moore et al., 1993), but have differing fluorescence intensities and lifetimes. As such, *a priori* it is preferable to use the mant derivative of 2′-deoxy-ATP, where the fluorophore is specifically located at the 3′ position. However, while the affinity of the Rep monomer for 3′-mant-dATP is lower than for 2′(3′)-mantATP, the kinetic *mechanism* of binding appears to be the same for both nucleotides (Figure 6A−C). Furthermore, the observed biphasic kinetics is not a consequence of the mant isomerization equilibrium. The two phases of the fluorescence change are more clearly resolved with 2′(3′)-mantATP, and thus use of this analogue allows the elementary rate constants to be determined with greater precision.

Kinetic Mechanism of mant Nucleotide Binding to the Rep Monomer. On the basis of the observation that mantATP binding to Rep shows biphasic kinetics below ~4−5 μM mantATP, a simple one-step bimolecular interaction of Rep with mantATP appears unlikely. Biphasicity in the kinetics of protein−ligand interactions can result from a variety of kinetic mechanisms, where the first phase reflects the bimolecular step and the second phase generally reflects first-order rearrangements of the protein, ligand, or both [see Johnson (1992), Halford (1971, 1972), and Bagshaw et al. (1974)]. Whereas mechanisms that involve an isomerization of the free enzyme (Engelborghs & Eccleston, 1982) or substrate (Trentham et al., 1969) prior to ligand binding are inconsistent with our experimental data [see Halford (1971, 1972)], we cannot rigorously exclude a mechanism involving two distinct binding modes for mantATP [see eq 19 of Bagshaw et al. (1974)]. However, this alternative mechanism is unlikely for ADP and AMPPNP binding to Rep, since it would require these nucleotides to have bimolecular association rate constants of ~10^5 M^{-1} s^{-1} (Moore & Lohman, 1994), which is uncharacteristically low for a bimolecular association rate constant (typically ~10^7−10^8 M^{-1} s^{-1}). As a result, Scheme 1 is the simplest mechanism that is consistent with the kinetic data for all of the nucleotides studied here and in the accompanying paper (Moore & Lohman, 1994). The ambiguities noted above in the interpretation of these data are inherent generally to systems where mechanisms analogous to Scheme 1 have been proposed.

As in the case of Rep, previous studies of a number of ATPases and GTPases have concluded that nucleotide binding proceeds by a two-step reaction mechanism [see Eccleston et al. (1992) and references therein]. Most often, this has been based on the hyperbolic (or at least nonlinear) dependence of the rate of nucleotide binding on substrate concentration. In these cases, the weak initial binding step has been assumed to be rapidly reversible and/or spectroscopically silent, such that only the conformational step was observed. However, with Rep, the initial binding of mantATP ($k_{obs,1}$) is observable on the stopped-flow time scale as a result of the slow dissociation of mantATP from the initial binary complex, P−mantATP, and thus we can determine all four rate constants describing Scheme 1.

Binding of mantATPγS, mantAMPPNP, and mantADP to the Rep Monomer. In studies of the kinetic mechanism of many ATPases and GTPases, nonhydrolyzable or slowly hydrolyzable nucleoside triphosphate analogues, such as AMPPNP and ATPγS, are commonly used to distinguish those steps associated with ligand binding from those that result from cleavage of the γ-phosphate. In general, we find that the kinetics and thermodynamics of mantATPγS binding to the Rep monomer (Figure 5A) are similar to those observed with mantATP; modification of the terminal phosphate leads to only a marginal reduction in overall binding affinity (Table 1). The ss-DNA-stimulated ATPγSase activity of Rep is ~10^3-fold lower than that observed with ATP under these conditions (K.J.M.M. and T.M.L., unpublished data). Therefore, ATPγS and its derivatives should be useful analogues of ATP for use in kinetic studies of the DNA-stimulated ATPase of Rep.

In contrast, the kinetics and thermodynamics of mantAMPPNP binding to Rep are very different from those of mantATP. A two-step binding mechanism for mantAMPPNP is inferred from the hyperbolic dependence of the observed rate constant on [mantAMPPNP] (Figure 5B, inset). It is unclear whether these two steps are the same as those observed for mantATP and mantATPγS (with different rates and equilibrium constants) or whether they have a different molecular origin. Clearly, a kinetic study cannot make this distinction unambiguously. Although there is evidence for a more tightly bound species from cold chase displacement experiments, apparently it is not highly populated at equilibrium. In this context, the parent nucleotide analogue, AMPPNP, which interacts with Rep in a manner very similar to that observed with mantAMPPNP, shows direct evidence for an additional bound state, (P−AMPPNP)** (Moore & Lohman, 1994). Despite the altered kinetics and thermodynamics of mantAMPPNP binding to Rep, the use of AMPPNP over ATPγS is preferable for equilibrium binding studies since the latter nucleotide is hydrolyzed at a low, but significant, rate by Rep. In our previous studies of the effects of nucleotides on the equilibrium DNA binding of Rep, high concentrations of AMPPNP (2 mM) were used (Wong & Lohman, 1992), so that saturation of the protein

with AMPPNP was likely to have been achieved despite its lower overall binding affinity for Rep.

The affinity of the Rep monomer for mantADP is significantly lower than for mantATP, although the binding mechanism also appears to be a two-step reaction (Figure 6D). In contrast, the DnaB helicase binds fluorescent analogues of ATP and ADP with comparable affinity (Biswas et al., 1986; Bujalowski & Klonowska, 1993). While the association rate constants are near 10^7 M^{-1} s^{-1} for Rep binding to both mantATP and mantADP, the dissociation rate constants (k_{-1} and k_{off}) for mantADP are ~30-fold and ~20-fold higher, respectively. Weaker binding of mantADP is also evident from the single-turnover hydrolysis of mantATP to mantADP, which leads to a net dissociation of nucleotide from Rep and is consistent with an overall affinity of ~10^6 M^{-1} for mantADP (see Figure 9). Due to the smaller fluorescence signals, weak binding, and rapid dissociation of mantADP from Rep, we have found it more convenient to monitor ADP binding indirectly by kinetic competition with mantATP (Moore & Lohman, 1994); the results of these experiments support the major conclusions discussed above.

Binding of mantATP to Rep at Higher Temperatures. The majority of the experiments reported here were performed under the same solution conditions and temperature (4 °C) used in the previous equilibrium studies of Rep−DNA binding (Wong et al., 1992; Wong & Lohman, 1992). However, since the kinetics of duplex DNA unwinding is generally performed at higher temperatures (Amaratunga & Lohman, 1993), we also investigated the binding kinetics of mantATP and 3′-mant-dATP as a function of temperature from 4 to 25 °C (Table 2). We observe that all four rate constants increase with increasing temperature. The apparent activation energy for the association step with rate constant k_{+1} is *ca.* + 10 kcal mol^{-1}, which is larger than that predicted for a diffusion-controlled reaction in 10% (v/v) glycerol (~6.5 kcal mol^{-1}).[3] At 25 °C in the presence of 5 mM Mg^{2+}, the bimolecular rate constant $k_{+1} = 4 \times 10^7$ M^{-1} s^{-1}, which is comparable to, or higher than, the bimolecular rate constants for other small ligands binding to proteins (Gutfreund, 1972; Fersht, 1985; Berg & von Hippel, 1985; Lohman, 1986); however, k_{+1} increases further upon removal of Mg^{2+}, indicating that these are not diffusion-controlled reactions.

While the equilibrium constant for the initial binding step, K_1, decreases with increasing temperature ($\Delta H° < 0$), the equilibrium constant for the second step is relatively independent of temperature. Therefore, the reduction in the overall equilibrium binding affinity of mantATP for Rep with increasing temperature is primarily due to changes in K_1 (Table 2). The effective rate of nucleotide dissociation, k_{off}, is likely to be too fast above 15 °C to permit nucleotide binding to be determined quantitatively by nonequilibrium separation methods, such as spin columns [upper limit ~0.2 s^{-1} for the nucleotide dissociation rate (Stitt, 1988)].

Effect of Mg^{2+} on mantATP Binding to the Rep Monomer. A divalent metal ion (e.g., Mg^{2+}) is required for Rep ATPase activity, although previous studies had not established whether Mg^{2+} is required for ATP binding *per se*. The data presented in Figure 7 indicate that the Rep monomer is able to bind Mg^{2+}-free mantATP (and also Mg^{2+}-free ATP; Moore & Lohman, 1994), although all four elementary rate constants are increased relative to those observed in the presence of excess [Mg^{2+}]. In particular, we observe that k_{+1} increases to a value of ~8×10^7 M^{-1} s^{-1} (at 4 °C), which is approaching that for a diffusion-controlled reaction (Berg & von Hippel, 1985; Lohman, 1986).

Scheme 5

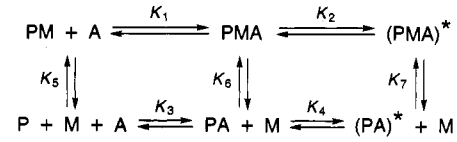

The mechanism of Mg^{2+} release from several protein−Mg^{2+}−nucleotide complexes has been studied by determining the effect of EDTA on the rate of nucleotide dissociation. Mechanisms analogous to Scheme 2 apply for EF-Tu (Eccleston, 1981) and $p21^{ras}$ (John et al., 1993), while a mechanism analogous to Schemes 3 and 4 describes the dissociation of nucleotides from myosin S-1 (Bagshaw & Trentham, 1974). The data presented here suggest that an intermediate situation occurs with Rep monomer, such that both the Mg^{2+} and the nucleotide dissociate from a P*−Mg^{2+}−mantATP complex at comparable rates. The much faster rate of Mg^{2+} dissociation from P*−Mg^{2+}−mantATPγS suggests that Mg^{2+} exerts its effect at the nucleotide binding site and may reflect the weaker interaction of sulfur with Mg^{2+} or possibly a less specific structural modification of the ATP binding site upon thio substitution.

The overall affinity of Rep for mantATP in the absence of Mg^{2+} ($K_{overall} = K_1K_2 \sim 2.5 \times 10^5$ M^{-1}) is ~10^3-fold lower than in the presence of Mg^{2+}, due to a ~10- and ~100-fold reduction in the values of K_1 and K_2, respectively. A thermodynamic cycle showing the interaction of Rep monomer (P) with mantATP (A) and Mg^{2+} (M) is shown in Scheme 5, where PMA* is equivalent to (P−mantATP)* in Scheme 1 and K_n is the equilbrium association constant for step n, with $K_1 = 3.4 \times 10^6$ M^{-1}, $K_2 = 73$, $K_3 = 3.3 \times 10^5$ M^{-1}, and $K_4 = 0.84$. Since $K_5K_1 = K_3K_6$ and $K_6K_2 = K_4K_7$, then $K_6 \sim 10K_5$ and $K_7 \sim 80K_6$. Thus, the affinity of Mg^{2+} for Rep increases in progression from P to P−mantATP to (P−mantATP)*. The accurate determination of K_5, K_6, and K_7, as well as the rate constants for these steps, will require more direct approaches to monitor Mg^{2+} binding. Such studies can also address the issue of whether there are additional binding sites for Mg^{2+} (or other metal ions) and help to determine the kinetically preferred path for the binding of a mixture of Mg^{2+} and ATP to metal-ion-free Rep.

The 10^3-fold reduction in the affinity of Rep for mantATP upon the removal of Mg^{2+} may reflect important interactions of Mg^{2+} with the triphosphate moiety of mantATP. We note that Rep−Mg^{2+} binds to inorganic phosphate more tightly than it does to adenosine (Moore & Lohman, 1994), suggesting that the interactions of Rep with the base and the ribose moiety of nucleotides are less important than those with the phosphate groups. Furthermore, UTP, GTP, and CTP bind with only 30−100-fold lower affinities than ATP (Arai et al., 1981a). The isomerization of P−Mg^{2+}−

[3] As calculated from the temperature dependence of the solution viscosity, a diffusion-controlled reaction in water is predicted to have an activation energy (E_{act}) of 4−5 kcal mol^{-1} (Lohman, 1986), whereas in 100% glycerol E_{act} is ~16 kcal mol^{-1} and in 10% glycerol E_{act} is predicted to be ~6.5 kcal mol^{-1}.

mantATP to (P−Mg^{2+}−mantATP)* is associated with an ~80-fold increase in affinity of the protein for Mg^{2+}. One possible explanation for these data is that the formation of the tightly bound complex may involve a relatively slow conformational change in the phosphate binding loop of Rep. Upon removal of the metal ion, we note that both forward rate constants increase. A model in which the binding of Mg^{2+} by Rep provides structural and conformational constraints on the protein (into a more closed conformation?) would be consistent with a reduction in the rates of all four rate constants relative to those obtained with Mg^{2+}-free Rep.

Intrinsic ATPase Activity of the Rep Monomer. Single-turnover kinetic experiments demonstrate that the Rep monomer possesses a slow, but significant intrinsic (DNA-independent) ATPase activity, which is independent of the Rep preparation (Figure 9). As a result, it is more appropriate to refer to the ATPase activity of Rep as DNA-stimulated rather than DNA-dependent. In fact, similar studies with other helicases will likely indicate that these NTPase activities are not strictly dependent upon DNA binding. The apparent steady-state rate of ATP hydrolysis measured with Rep in the absence of added DNA is slightly Rep preparation-dependent and is faster than the true first-order cleavage rate measured in our single-turnover experiments, and thus it must represent an overestimation of the true k_{cat}. This higher value for k_{cat} determined from a steady-state ATPase measurement probably reflects the presence of low, but variable, amounts of contaminating DNA, which dramatically increases the *apparent* steady-state rate of ATP hydrolysis. Since we observe no burst of product formation in these multiple-turnover experiments, it is likely that the rate-limiting step in the Rep monomer ATPase occurs either prior to or at the chemistry step. Although the intrinsic rate of ATP hydrolysis by Rep monomer is slow (~0.001 s^{-1} at 4 °C, ~0.01 s^{-1} at 25 °C), it is >50-fold faster than the intrinsic GTPase activity of $p21^{ras}$ (Neal et al., 1988; Moore et al., 1993). The intrinsic ATPase activity of Rep increases by ~10^3-fold upon ss-DNA binding and by an additional ~10-fold upon Rep dimerization (Wong et al., 1993; K.J.M.M., unpublished experiments). An understanding of the mechanism by which the binding of DNA and the subsequent dimerization of Rep increase the intrinsic ATPase by ~10^4-fold remains an important goal for future studies.

Equilibrium binding of nucleotides to Rep (Arai et al., 1981a) and other helicases has been studied in the absence of nucleic acids, e.g., *E. coli* DnaB (Arai et al., 1981b; Biswas et al., 1986; Bujalowski & Klonowska, 1993) and *E. coli* rho protein (Stitt, 1988; Geiselmann & von Hippel, 1992); however, this report is the first to consider the detailed kinetics of nucleotide binding. Our results also suggest an explanation for why a Rep−ATP complex was not observed in the absence of Mg^{2+} by Arai et al. (1981a). Under these conditions, the rate of nucleotide dissociation from Rep is rapid (e.g., Figure 8C) on the time scale of the separation procedure used (filter binding); hence, the inability to observe nucleotide complex formation is likely to be a kinetic artifact of the separation technique. A similar explanation likely applies to the inability to observe the binding of ATP to rho by ultrafiltration techniques (Stitt, 1988).

In summary, the data presented here are consistent with the two-step mechanism shown in Scheme 1 for the binding of mantATP to the Rep monomer. Furthermore, the kinetics and equilibrium binding properties of the Rep monomer are modulated dramatically by Mg^{2+} in ways that suggest important interactions of the triphosphate moiety of mantATP with the Mg^{2+} ion. In the Rep system, the mant derivative of ATPγS appears to be a better kinetic analogue of mantATP than does mantAMPPNP. The use of mantATP to determine the kinetic and equilibrium parameters for the interaction of Rep with nonfluorescent ligands by kinetic competition methods is described in the accompanying paper (Moore & Lohman, 1994). Both approaches should prove useful for subsequent studies of the nucleotide binding and hydrolysis properties of the different Rep−DNA dimer species (Wong et al., 1992) and of other helicases.

ACKNOWLEDGMENT

We thank Dr. N. Millar (KSIM, KFIT) and Dr. C. Frieden (KINSIM, FITSIM) for the data simulation and fitting programs, Bill van Zante for technical assistance, and K. Bjornson, J. Ali, and M. Ferrari for their comments.

REFERENCES

Amaratunga, M., & Lohman, T. M. (1993) *Biochemistry 32*, 6815−6820.

Arai, N., & Kornberg, A. (1981) *J. Biol. Chem. 256*, 5294−5298.

Arai, N., Arai, K. I., & Kornberg, A. (1981a) *J. Biol. Chem. 256*, 5287−5293.

Arai, K. I., Yasuda, S. L., & Kornberg, A. (1981b) *J. Biol. Chem. 256*, 5247−5252.

Bagshaw, C. R., & Trentham, D. R. (1974) *Biochem. J. 141*, 331−349.

Bagshaw, C. R., Eccleston, J. F., Ekstein, F., Goody, R. S., Gutfreund, H., & Trentham, D. R. (1974) *Biochem. J. 141*, 351−364.

Barshop, B. A., Wrenn, R. F., & Frieden, C. (1983) *Anal. Biochem. 130*, 134−145.

Berg, O. G., & von Hippel, P. H. (1985) *Annu. Rev. Biophys. Biophys. Chem. 14*, 131−160.

Bernasconi, C. F. (1976) in *Relaxation Kinetics*, Academic Press, New York.

Biswas, E. E., Biswas, S. B., & Bishop, J. E. (1986) *Biochemistry 25*, 7368−7374.

Brownbridge, G. G., Lowe, P. N., Moore, K. J. M., Skinner, R. H., & Webb, M. R. (1993) *J. Biol. Chem. 268*, 10914−10919.

Bujalowski, W., & Klonowska, M. M. (1993) *Biochemistry 32*, 5888−5900.

Chao, K., & Lohman, T. M. (1990) *J. Biol. Chem. 265*, 1067−1076.

Chao, K., & Lohman, T. M. (1991) *J. Mol. Biol. 221*, 1165−1181.

Colasanti, J., & Denhardt, D. T. (1987) *Mol. Gen. Genet. 209*, 382−390.

Cremo, C. R., Neuron, J. M., & Yount, R. G. (1990) *Biochemistry 29*, 3309−3319.

Daniels, D. L., Plunkett, G., Burland, V., & Blattner, F. R. (1992) *Science 257*, 771−778.

Denhart, D. T., Dressler, D. H., & Hathaway, H. (1967) *Proc. Natl. Acad. Sci. U.S.A. 57*, 813−820.

Eccleston, J. F. (1981) *Biochemistry 20*, 6265−6272.

Eccleston, J. F., Moore, K. J. M., Brownbridge, G. G., Webb, M. R., & Lowe, P. N. (1991) *Biochem. Soc. Trans. 19*, 432−436.

Eccleston, J. F., Gutfreund, H., Trentham, D. R., & Webb, M. R. (1992) *Philos. Trans. R. Soc. London B 336*, 1−112.

Eccleston, J. F., Moore, K. J. M., Morgan, L., Skinner, R. H., & Lowe, P. N. (1993) *J. Biol. Chem. 268*, 27012−27019.

Engelborghs, Y., & Eccleston, J. F. (1982) *FEBS Lett. 141*, 78–81.
Fersht, A. R. (1985) in *Enzyme Structure and Mechanism*, Freeman, San Francisco.
Geiselmann, J., & von Hippel, P. H. (1992) *Protein Sci. 7*, 850–860.
Gilchrist, C. A., & Denhart, D. T. (1987) *Nucleic Acids Res. 15*, 465–475.
Gutfreund, H. (1972) in *Enzymes*: Physical *Principles*, Wiley (Interscience), New York.
Halford, S. E. (1971) *Biochem. J. 125*, 319–327.
Halford, S. E. (1972) *Biochem. J. 126*, 727–738.
Hill, T. L., & Tsuchiya, T. (1981) *Proc. Natl. Acad. Sci. U.S.A. 78*, 4796–4800.
Hiratsuka, T. (1983) *Biochim. Biophys. Acta 742*, 496–508.
Hodgman, T. C. (1988) *Nature (London) 333*, 22–23.
John, J., Sohmen, R., Feuerstein, J., Linke, R., Wittinghofer, A., & Goody, R. S. (1990) *Biochemistry 29*, 6058–6065.
John, J., Rensland, H., Schlichting, I., Vetter, I., Borasio, G. D., Goody, R. S., & Wittinghofer, A. (1993) *J. Biol. Chem. 268*, 923–929.
Johnson, K. A. (1992) in *The Enzymes*, pp 1–61, Academic Press, Inc., New York.
Kornberg, A., Scott, J. F., & Bertsch, L. L. (1978) *J. Biol. Chem. 253*, 3298–3304.
Lane, H. E. D., & Denhart, D. T. (1974) *J. Bacteriol. 120*, 805–814.
Lane, H. E. D., & Denhart, D. T. (1975) *J. Mol. Biol. 97*, 99–112.
Lohman, T. M. (1986) *CRC Crit. Rev. Biochem. 19*, 191–245.
Lohman, T. M. (1992) *Mol. Microbiol. 6*, 5–14.
Lohman, T. M. (1993) *J. Biol. Chem. 268*, 2269–2272.
Lohman, T. M., Chao, K., Green, J. M., Sage, S., & Runyon, G. (1989) *J. Biol. Chem. 264*, 10139–10147.
Matson, S. W. (1991) *Prog. Nucleic Acid Res. 40*, 289–326.
Matson, S. W., & Kaiser-Rogers, K. A. (1990) *Annu. Rev. Biochem. 59*, 289–329.
Moore, K. J. M. (1992) Ph.D. Thesis, University of London, London, U.K.
Moore, K. J. M., & Lohman, T. M. (1994) *Biochemistry 33*, 14565–14578.
Moore, K. J. M., Webb, M. R., & Eccleston, J. F. (1993) *Biochemistry 32*, 7451–7459.
Neal, S. E., Eccleston, J. F., Hall, A., & Webb, M. R. (1988) *J. Biol. Chem. 263*, 19718–19722.
Neal, S. E., Eccleston, J. F., & Webb, M. R. (1990) *Proc. Natl. Acad. Sci. U.S.A. 87*, 3562–3565.
Rensland, H., Wittinghofer, A., & Goody, R. S. (1991) *Biochemistry 30*, 11181–11185.
Sadu, A., & Taylor, E. W. (1992) *J. Biol. Chem. 267*, 11352–11359.
Scott, J. F., Eisenberg, S., Bertsch, L. L., & Kornberg, A. (1977) *Proc. Natl. Acad. Sci. U.S.A. 74*, 193–197.
Stitt, B. L. (1988) *J. Biol. Chem. 263*, 11130–11137.
Thommes, P., & Hubscher, U. (1992) *Chromosoma 101*, 467–473.
Trentham, D. R., McMurray, C. H., & Pogson, C. I. (1969) *Biochem. J. 114*, 19–28.
Walker, J. E., Saraste, M., Runswick, M. J., & Gay, N. J. (1982) *EMBO J. 1*, 945–951.
Washburn, B. K., & Kushner, S. R. (1991) *J. Bacteriol. 173*, 2569–2575.
Wong, I., & Lohman, T. M. (1992) *Science 256*, 350–355.
Wong, I., Chao, K. L., Bujalowski, W., & Lohman, T. M. (1992) *J. Biol. Chem. 267*, 7596–7610.
Wong, I., Amaratunga, M., & Lohman, T. M. (1993) *J. Biol. Chem. 268*, 20386–20391.
Woodward, S. K. A., Eccleston, J. F., & Geeves, M. A. (1991) *Biochemistry 30*, 422–430.
Yarranton, G. T., & Gefter, M. L. (1979) *Proc. Natl. Acad. Sci. U.S.A. 76*, 1658–1662.
Zimmerle, C. T., & Frieden, C. (1989) *Biochem. J. 258*, 381–387.
Zimmerle, C. T., Patane, K., & Frieden, C. T. (1987) *Biochemistry 26*, 6545–6552.